MULTISCALE MODELLING OF ADHESIVE JOINTS WITH NANO FILLERS

By

Sana Ijaz

(Registration No: 00000364368)

Department of Mechanical Engineering

School of Mechanical and Manufacturing Engineering

National University of Sciences & Technology (NUST)

Islamabad, Pakistan

(2024)

MULTISCALE MODELLING OF ADHESIVE JOINTS WITH NANO FILLERS

By

Sana Ijaz

(Registration No: 00000364368)

A thesis submitted to the National University of Sciences and Technology, Islamabad,

in partial fulfillment of the requirements for the degree of

Master of Science in
Mechanical Engineering

Supervisor: Dr. Aamir Mubashar

School of Mechanical and Manufacturing Engineering

National University of Sciences & Technology (NUST)

Islamabad, Pakistan

(2024)

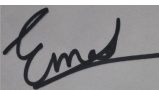# THESIS ACCEPTANCE CERTIFICATE

Certified that final copy of MS/MPhil thesis written by **Regn No. 00000364368 Sana Ijaz** of **School of Mechanical & Manufacturing Engineering (SMME)** has been vetted by undersigned, found complete in all respects as per NUST Statues/Regulations, is free of plagiarism, errors, and mistakes and is accepted as partial fulfillment for award of MS/MPhil degree. It is further certified that necessary amendments as pointed out by GEC members of the scholar have also been incorporated in the said thesis titled. **Multiscale Modelling of Adhesives with Nano Fillers**

Signature: ⎯

Name (Supervisor): Aamir Mubashar

Date: 19 - Mar - 2024

Signature (HOD): ⎯

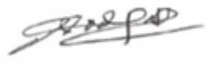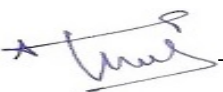**Date:** 19 - Mar - 2024
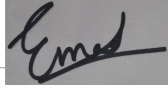
Signature (DEAN): ⎯

Date: 19 - Mar - 2024

National University of Sciences & Technology (NUST)

MASTER'S THESIS WORK

We hereby recommend that the dissertation prepared under our supervision by: <u>Sana Ijaz (00000364368)</u>

Titled: <u>Multiscale Modelling of Adhesives with Nano Fillers</u> be accepted in partial fulfillment of the requirements for the award of <u>MS in Mechanical Engineering</u> degree.

Examination Committee Members

1. Name: Sadaqat Ali   Signature:

2. Name: Emad Ud Din   Signature:

Supervisor: Aamir Mubashar   Signature:

Date: <u>19 - Mar - 2024</u>

<u>19 - Mar - 2024</u>

Head of Department   Date

COUNTERSINGED

<u>19 - Mar - 2024</u>

Date   Dean/Principal

AUTHOR'S DECLARATION

I Sana Ijaz hereby state that my MS thesis titled "Multiscale Modelling of Adhesive Joints with Nano Fillers" is my own work and has not been submitted previously by me for taking any degree from National University of Sciences and Technology, Islamabad or anywhere else in the country/ world.

At any time if my statement is found to be incorrect even after I graduate, the university has the right to withdraw my MS degree.

Name of Student:＿＿＿＿＿＿ Sana Ijaz ＿＿＿＿＿

Date: ＿＿＿＿ 26-03-2024 ＿＿＿＿＿＿＿＿＿＿＿

PLAGIARISM UNDERTAKING

I solemnly declare that research work presented in the thesis titled "Multiscale Modelling of Adhesive Joints with Nano Fillers" is solely my research work with no significant contribution from any other person. Small contribution/ help wherever taken has been duly acknowledged and that complete thesis has been written by me.

I understand the zero tolerance policy of the HEC and National University of Sciences and Technology (NUST), Islamabad towards plagiarism. Therefore, I as an author of the above titled thesis declare that no portion of my thesis has been plagiarized and any material used as reference is properly referred/cited.

I undertake that if I am found guilty of any formal plagiarism in the above titled thesis even after award of MS degree, the University reserves the rights to withdraw/revoke my MS degree and that HEC and NUST, Islamabad has the right to publish my name on the HEC/University website on which names of students are placed who submitted plagiarized thesis.

Student Signature:

Name: Sana Ijaz

Dedicated to my exceptional parents, adored siblings and encouraging husband whose tremendous support and cooperation led me to this wonderful accomplishment.

ACKNOWLEDGEMENTS

I am thankful to my Creator Allah Subhana-Watala to have guided me throughout this work at every step and for every new thought which You setup in my mind to improve it. Indeed I could have done nothing without Your priceless help and guidance. Whosoever helped me throughout the course of my thesis, whether my parents or any other individual was Your will, so indeed none be worthy of praise but You.

I am profusely thankful to my beloved parents who raised me when I was not capable of walking and continued to support me throughout in every department of my life. For their unwavering support, boundless love, and the sacrifices they made to ensure my journey through education was paved with encouragement and opportunity. Their belief in my abilities has been the cornerstone of my achievements.

I would also like to pay special thanks to my husband for his enduring love, understanding, and constant encouragement. His belief in my dreams and his steadfast presence have been my greatest blessings. Together, we have weathered challenges and celebrated triumphs, making this academic journey even more meaningful.

I would also like to express special thanks to my supervisor Aamir Mubashar for his help throughout my thesis and also for CFD and Non-Linear Dynamics courses which he has taught me. I can safely say that I haven't learned any other engineering subject in such depth than the ones which he has taught.

Finally, I would like to express my gratitude to all the individuals who have rendered valuable assistance to my study.

TABLE OF CONTENTS

LIST OF TABLES

Page No.

LIST OF FIGURES

Page No.

ABSTRACT

The study examines the strength and durability of single lap joint created using the identical epoxy adhesives (LY-556/AD 22962) that are single lap adhesively joined. As per credible research data available, epoxy adhesives and single lap adhesively bonded joints' failure strengths are influenced by a number of factors, and their strength can be increased using a number of different techniques. Addition of filler material to epoxy is one of the efficient techniques. A flexible natural raw material, cork powder is used to strengthen adhesives and SLJs that are adhesively bonded by acting as a crack-stopping filler. However, with change in concentration of filler, this behavior of cork powder changes.

The current work focuses on evaluating differences in the structural characteristics of epoxy-based adhesives and adhesively bonded single lap joints at various temperatures and cork powder concentrations. A series of simulation have been performed for investigation of SLJs strength with LY-556 as epoxy adhesive and Aluminum 5052 as adherend. The adhesively bonded joint is tested at different temperature ranges from 25ºC, 50ºC, 75ºC and 100ºC with the concentration of cork powder ranging from weight percentages of 0.25, 0.5, 0.75 and 1.

Keywords:

Multiscale modelling, adhesives, nano-fillers, strength, stiffness, durability

CHAPTER 1: INTRODUCTION

1.1 Motivation

Adhesives were part of the industrial revolution that started in the mid-18th century and they have played a significant part in joining wooden pieces for bridges, aircrafts and ships (Utracki et al., 2013). But compared to adhesives, metallic structures provided more stability and lower fatigue effects. But with metallic structures came along fasteners, bolts and rivets that contributed heavily to the weight of the structure resulting in more fuel usage for vehicles and other moving vessels.

To overcome this liability of the metallic joints, adhesively bonded joints were introduced that included the adherend and the adhesive. After solidifying, the adherend and adhesive bond in an adhesive joint promises mechanical integrity and in turn contributes to increased strength and reduced stress singularity in the joined structure (He et al., 2011). Adhesive bonding in place of metallic fastener is also crucial because in order to reduce structural damage, joint failure need to be reduced for which improved stiffness of the joint is required. Adhesive joints also contribute in weight reduction of the joint (about 10-30% as compared to mechanical joints), better sealing properties, increased stiffness of the joint, increased degradation resistance because of corrosion/erosion and enhanced fatigue strength (Nemati Giv et al., 2018).

With all the mentioned benefits above, it is imperative to explore the field of adhesive joints but keeping in view the modern practices of designing that is multiscale modelling and simulation. Multiscale modelling helps in capturing system complexity, improved accuracy, increased efficiency of the simulation products, getting insight into emergent properties of the materials that only appear at certain length scales (e.g., nano) and risk assessment and prediction as per boundary conditions and varying loading conditions.

1.2 Selection of Adhesives and Methodology

Selection of adhesive depends on three checks that include adhesive property check, adhesive application requirement checks and curing requirement check. After all of

the above-mentioned checks, an adhesive is fit to be used for improved strength and structural integrity.
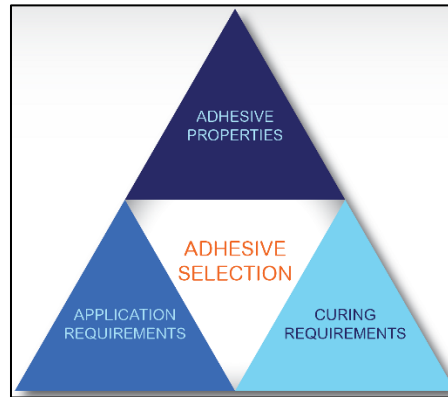
Figure 1.1: Selection of Adhesive Criteria (Suárez et al., 2003)

Among the adhesive properties lie substrate type, adhesive form, manufacturing needs and constraints, cost and pre-treatment. Joint performance requirements are also crucial in this selection process and they include loading type on the adherend, load magnitude and periodicity, unique properties i.e., conductivity of the adhesive and adherend, operating environment of the joint and durability of the joint.

Application requirement check includes aesthetics, joint/structure design as well as testing and validation. Curing requirements check keeps in view the fabrication issues i.e., curing, jigging, dispensing and controlling the environment. All of these checks contribute towards the selection of an adhesive that will present useful results in the scope of this research.

For selection of a modelling methodology, it should be kept in mind that multiscale modelling is a useful tool for studying materials at several length scales, from the atomic to the macroscopic. Because of its capacity to forecast the behavior of materials under diverse loading circumstances and optimize their qualities for specific applications, it has become more popular in domains such as aerospace, automotive, and construction (Van Der Giessen et al., 2020). Because of their superior mechanical and interfacial qualities, nano-filler adhesive materials have gained a lot of interest in recent years. The inclusion of

nano-fillers such as graphene oxide, carbon nanotubes, and nanoparticles can considerably improve the adhesive material's stiffness, strength, and toughness.

Finite Element Modelling (FEM) is a powerful computational method that is being used in engineering for quite some time now and is improving day by day as the complexity of the structures. FEA offers several benefits that include design optimization by providing insights into how factors like materials, geometry and loads affect the performance or behavior of a structure (Fang et al., 2017). It also provides a cost-efficient solution because simulation, tests and designs are all virtually performed as well as increased product reliability because the defects and deformities are diagnosed at an earlier stage leading to better results optimization. FEA also provides multi-physics analysis such as structural, thermal, electromagnetic, and fluid dynamics that play such a crucial role in modern industry and development.

1.3 Adhesive Joint Characterization

An adaptable approach, adhesive bonding, used in many engineering as well as manufacturing applications, offers a variety of adhesive joints that can be customized to meet particular needs. This section describes in detail the primary types of adhesive joints, such as lap joints, butt joints, T-joints, and scarf joints, as well as their respective qualities, advantages, and applications.

1.3.1 Lap Joints:

Among the many prominent types of adhesive joints is the lap joint, which occurs when two adherends partially overlap. Lap joints are ideal for applications needing strength against shear because they disperse loads uniformly over the bond surface. In regards to stress distribution and load carrying ability, the adhesive bond improves the adherends by transferring load among them. In the aerospace sector, lap joints are frequently utilized for bonding body panels on aircraft as well as for the construction of aircraft parts (Shang et al., 2019).

Lap joints include orientations such as single lap joints, beveled lap joint, joggle lap joint, single strap lap joint, double strap lap joint, recessed double strap lap joint,

3

beveled double strap lap joint, strap lap joint, double lap joint and tongue and groove lap joint. All these configurations provide different type of structural integrity and have various applications in different industries.

1.3.2 Butt Joints:

Two adherends are bonded end to end without overlapping in butt joints. These joints stand out for having little adhesive bond surface. Because of their low profile, butt joints are especially useful when aesthetics and a flush, smooth look are required (Alwar et al., 1976). To achieve the required structural strength, they could, however, need more mechanical attachments. Butt joints are used in the construction of furniture, cabinets, and architectural components.

Butt joints include straight/plain butt joint (the most common type), single V, single U, double V, double U, double bevel orientations etc.

1.3.3 T-Joints:

T-joints are formed when two adherends meet at a right angle, forming the shape of the letter "T." These joints have an excellent load-carrying capability both in the shear and tensile regimes and are frequently employed in structural applications (Carneiro et al., 2017). T-joints are widely used in construction for connecting columns and beams utilizing adhesive bonding methods, which lower stress concentrations at the joints and ensure structural stability.

1.3.4 Scarf Joints:

Scarf joints are made with an adherend overlap that is angled and tapered, resembling a wedge. By using this design, the adhesive bond area is increased and the joint's ability to support more weight is improved. Scarf joints are useful in situations where high strength and even stress distribution is necessary, such as in the maritime sector for connecting boat hulls and aircraft parts (Lubkin et al., 1957). Scarfed butt joints are the most common type in which two tapered surfaces are joined face-to-face resulting in more bonded area and increased strength.

When comparing all these types, engineers and designers use various configurations on the application area of the joint but the most commonly used configuration is that of a single lap joint (SLJ). SLJs are extensively used in major structural elements and members that bear load of various assemblies because SLJs are simple and reliable.

1.4 Usage of Adhesives

Adhesives are utilized in a variety of applications, ranging from home repairs to aerospace engineering. Adhesives are a quick and inexpensive way to attach dissimilar materials, reducing the need for traditional mechanical fasteners like screws and bolts (Kellar et al., 2021). Adhesives can also form a continuous connection across surfaces, distributing stresses more uniformly and resulting in greater load bearing capability. However, adhesive materials' behavior may be complicated, and their characteristics might vary depending on parameters such as the kind, size, and form of the adhesive, as well as the qualities of the substrates. Furthermore, the interfacial strength of the adhesive and the substrate might affect the total strength of the junction.

The inclusion of nano-fillers is one potential method for increasing the mechanical and interfacial characteristics of adhesive materials (Thabet et al., 2011). The unique qualities of these fillers, such as their large surface area, aspect ratio, and modulus, can greatly improve the adhesive material's properties. Carbon nanotubes, for example, have been demonstrated to boost the stiffness and strength of an epoxy glue by up to 100% and 50%, respectively (Sydlik et al., 2013). Similarly, adding graphene oxide to an epoxy glue can boost its hardness by up to 200% (Ferreira et al., 2018).

However, the behavior of adhesive materials containing nano-fillers can be complex, with properties varying depending on the kind, form, size, and concentration of the nano-fillers, the matrix material's properties, and the interactions at the interface that occur between the nano-fillers and the matrices (Sanghvi et al., 2022). As a result, studying the behavior of adhesive materials including nano-fillers involves the use of a multiscale modeling approach capable of representing interactions over various length scales.

5

1.5 Problem Statement

Improvement in overall strength of adhesive joints has been observed by addition of nano particles, moreover, predictive models that incorporate effects of strength improvement need more development, hence, a modelling and simulation approach is needed. The strength of single lap joints is enhanced by incorporation of nano particles at room temperature but behaviour of single lap joints with respect to durability is still unknown under various temperatures and different concentrations of nano particles.

Based on bisphenol-A, Araldite LY556, has medium viscocity and is an epoxy resin that is unmodified. With resistance to chemicals, it has excellent mechanical properties that can be varied within wide limits by usage of different hardeners and fillers at varying length scales e.g., micro, nano etc. Araldite has a low tendency to crystallization and is widely used in aircraft and aerospace adhesives. The strength of this adhesively bonded joint at different temperatures ranging from 25º, 50º, 75º and 100ºC is the interest of study here at different wt% of nano-particle fillers e.g., 0, 0.25,0.5,0.75 and 1.

1.6 Aim and Objectives

The aim of this study is to create a Finite Element Method-based model that can estimate the strength of single lap adhesive joints using different weight percentages (wt%) of nano particles. The following objectives were identified to achieve this aim:

a)   To analyze peel and shear stress at four different concentrations of the nano particle at four different temperatures.

b)   To compare the effect of adding cork powder into neat adhesive at different temperatures.

c)   To analyze the response of neat and cork powder added adhesive upon tensile loading.

1.7 Research Methodology

Many new methods for increasing the durability of structural adhesives have been developed in the previous few decades. Consequently, a review of the literature on methods for adding different nano- and microparticles to adhesives to increase their toughness was done. A summary of the main methods for toughening adhesives is provided, emphasizing the use of cork particles.

Moreover, adhesives behave in a more ductile but weaker manner under high temperatures and are more prone to creep but with low temperatures brittle behavior is observed where the strain to failure is low (Marques et al., 2015). Literature review covers such behavior of adhesives at varying temperatures.

Peel and shear stress profiles at different paths in the adhesive layer have been studied to access the influence of cork powder concentration (0, 0.25, 0.50, 0.75, 1 wt%) at various temperatures (25, 50, 75, 100C). Figure below shows different configurations in which the simulations were performed:
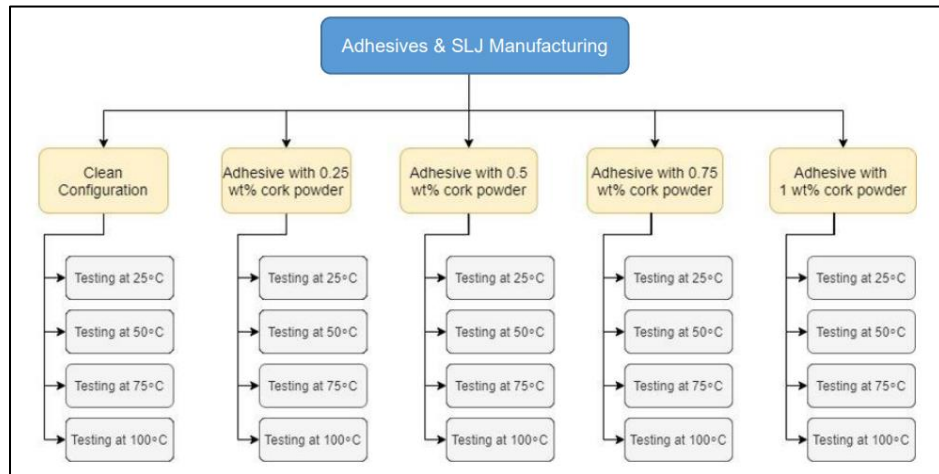
Figure 1.2 Schematic Diagram of Cork Specimens at different wt% and temperatures

ABAQUS CAE has been used to design the model of single lap joint and further analysis for peel and shear stress profiles has also been computed using the same software. Elastic stress analysis has been carried out for araldite LY556 + cork powder (adhesive) and Aluminium 5052. Validating the model through simulation of experimental data is the goal here.

CHAPTER 2: LITERATURE REVIEW

The present surge in multiscale modelling related to the study of solid mechanics, which has now evolved into a global interdisciplinary discipline affecting practically every industry, originated from an unexpected source. As the US Department of Energy (DOE) national labs began to reduce below ground nuclear tests in the middle of the 1980, with the last one in 1992, the idea of simulation-based technology as well as assessment ideas emerged, and multiscale modeling became critical in achieving improved accuracy and precision in prediction tools.

In their review of the concept of multiscale modeling, Horstemeyer and Mark state that multiscale modeling is a versatile tool that has many advantages such as shortening the duration of product development through the elimination of costly trial and error stages, lowering product costs through material, product, and workflow design Improvements assisting in cutting down of the amount of costly large-scale experiments, improving product quality and performance by predicting reaction to design pressures (Horstemeyer et al., 2010).

Beginning with the solid mechanics continuum theory framework, two fundamental multiscale approaches are available: hierarchical and concurrent. The bridging approach is the key differentiator (Steinhauser et al. 2017). The bridge approach in concurrent techniques is numerical or computational in nature. Hierarchical approaches run numerical computations separately at various length scales. Then, a bridge methodology, such as statistical analysis methods, homogenization techniques, or optimization methods, can be utilized to locate the important cause-effect correlations at the lower scale before determining the appropriate impacts at the higher scale.

For an even more impactful design and manufacturing through multiscale modelling, concurrent multiscale method's computational time must be on the order of the computation required for more accurate treatment using hierarchical methods. If this is not true, there is no point in using concurrent multiscale methods because hierarchical multiscale methods can be performed separately with shorter processing times. Certainly,

this limits the use of concurrent techniques to two- or three-dimensional scales, whereas hierarchical methods are not restricted to only two length scales.

Hu et al., (2010) in their research on carbon nanotubes used various multiscale modeling techniques to study nanotube array with gecko-like laterally dispersed tips. To assess the frictional and adhesive properties associated with this hierarchical fibrillar system, a multiscale modeling approach was developed. Coarse-grained molecular dynamics was employed to simulate a vertically oriented carbon nanotube array with horizontally distributed sections. The impact of horizontally dispersed sections on adhesive and friction strengths were studied and certified as cohesive laws for application in finite element modeling at unit scale. The findings suggest that horizontally distributed sections are crucial in producing considerable force anisotropy across the normal and shear axes in adhesives (Qu et al., 2008). The analysis of finite elements reveals a unique friction-enhanced adhesion process for the carbon nanotube array, that is additionally observed in the gecko adhesive system. The multiscale modeling method connects the carbon nanotube array's microlevel structures to its macrolevel adhesive behaviors, and the results shed light on the workings of gecko-mimicking dry adhesives.

Rothon et al. (1995) in their research described five basic characteristics of any particulate filler. These five characteristics remain same whether the particles are micro or nano. These include:

1)   What properties are being desired in the filling material?

2)   By the addition of fillers, what unwanted changes are possible and if these changes can be tolerated or not?

3)   How simple is the filler to work with and how may it effect the processing or simulation in this case?

4)   Is there a need for any special additives?

5)   What is the exact cost of utilizing a filler, is it acceptable and if there are any cheaper or dependable alternatives available?

The addition of high modulus particles increases the modulus of a polymeric material independent of particulate sizes; nevertheless, the stiffening influence may be stronger for particles that have greater aspect ratios. The modulus of particle-modified polymers can potentially be estimated using various theoretical approaches, including the Halpin-Tsai and Mori-Tanaka models (Ahmed et al., 1990). The aforementioned models have already been shown to be widely relevant to nanoparticle-modified polymers (Kinloch et al., 2006), however finite element modeling may produce more exact forecasts (Sheng et al., 2004). For precise predictions, the true aspect ratio of particles, the degree of alignment, and an understanding of the strength of adhesion among particle and polymer matrix are required. However, the elastic properties of nanoparticles are challenging to assess, hence they remain primarily unstudied. Nanoclays like montmorillonite are used (Vanorio et al. 2003). The absence of modulus data is due to the small particle size, thereby rendering accurate measurements impossible. As an outcome, the majority of authors believe that the nanoparticles' properties (e.g., modulus, density) are identical with those of the bulk material or a similar substance.

The addition of 3% carbon nanofibers (CNF) to an amine-cured epoxy polymer (Zhou et al. 2007) resulted in a 19% increase in modulus, demonstrating the stiffening effect that nanoparticles may give. This was followed by an increase in tensile strength and a decrease in strain at failure.

It has been shown that nanoparticles improve the structural and functional properties of thermoset polymers. Nonetheless, equal improvements may be achieved in many situations with micron-sized particles, particularly for structural properties. High aspect ratio particles, such as carbon nanotubes or nano-clay, can greatly improve functional properties (Hsieh et al. 2010). Electrical percolation at extremely low particle volume fractions and changes in barrier properties are two examples.

The most exciting issue right now is the synergistic effect of combining nanoparticles with existing micron-sized particle technologies (Brooker et al., 2010). Combining silica nanoparticles and rubber microparticles, for example, can boost the fracture toughness and

peel performance of adhesive junctions. These hierarchical materials, as well as organized arrays of nanoparticles, are expected to represent future advances in this field.

Upadhyaya et al. (2020) employ an Atomistic-based continuum (ABC) multiscale modeling technique to forecast the strength and failure of epoxy composite adhesives enhanced with carbon nanotubes (CNTs) in a bonded system. The mechanical characteristics of nanocomposite adhesives are determined using a two-step homogenization approach, with the assumption that CNT dispersion in the epoxy matrix is uniform. The first phase involves determining the mechanical characteristics of nanocomposites using the Representative Volume Element (RVE) approach.

Separated by an interphase, The RVE is made-up of a CNT placed into an epoxy matrix. An ABC modelling method is used to depict the structure-property link at the nanoscale, with a CNT regarded as a space-frame structure with beam components and the epoxy simulated using solid elements (Zare et al., 2015). Non-linear spring components are used to model the interphase between CNT and the epoxy, to account for non-bonded van der Waals forces. Into the following phase, CNT additions with various orientations in the matrix are investigated to produce a nanocomposite's microscale RVE. Varying boundary conditions have been applied to the RVEs in both stages, and finite element (FE) investigations were undertaken to evaluate the effective mechanical properties by numerical homogenization.

Al Mahmud et al. (2021) conducted study on the mechanical characteristics of epoxy adhesives, reinforcing epoxy nanocomposites with graphene nanoplatelets having functional group and without functional group. The study focused on Graphite nanoplatelet (GNP), extremely pure graphene oxide (GO), and graphene oxide - functionalized (FGO). The functional mechanical properties of the phase interphase areas of the three composite materials for nanotechnology were predicted using molecular dynamics (MD) with a reactive force field (ReaxFF). A systematic computational approach is developed to simulate strengthening nanoplatelets and examine their effects on the physical attributes of the epoxy.

With one atom thick and detect free sheet, Graphene is considered to be the best ever tested material. High specific surface area, unique graphitized plane structure, and high mobility of charges of graphene are the qualities of graphene that help in improving thermal, mechanical and electrical properties of polymers/adhesives (Lee et al., 2008). The scenario differs for nanoscale fillers or particles, such as graphene nanoplatelets and carbon nanotubes, which have a wide range of aspect ratios (Gao et al., 2017). Research findings to capture the influence for certain carbon nanofiller sizes (aspect ratio) often point to an improvement in the engineering characteristics of nanocomposites as the aspect ratio increases (Karevan et al., 2010). Unfortunately, experimental approaches are impracticable and limited to investigating the effect of aspect ratio in a reinforcing polymer matrix with nanoscale fillers. As a result, it is vital to fully understand the effects of changing the aspect ratio on polymer matrix properties.

Molecular dynamics (MD) technique has been used to simulate Graphene Nanoplatelets (GNP), Graphene Oxide (GO) and Functionalized Graphene Oxide (FGO) in a way that pure graphene is used as nanofiller in GNP while functional groups are randomly placed in both GO and FGO. All nanoplatelets (GNP, GO, and FGO) have continuous lateral edges (periodic boundary conditions). Because carboxyl and carbonyl are more likely to exist in low concentrations near the edges and in faulty regions (open rings or voids) in graphene nanoplatelets (Stankovich et al., 2006), their presence as functional groups in GO and FGO was overlooked. To account for any variation in predicted characteristics, five MD replicates of each nanoplatelet type (GNP, GO, and FGO) were simulated. The associated functional groups were randomly distributed in each MD duplicate of the GO and FGO. However, the chemical concentration and functional group composition of all GO and FGO MD duplicates were retained. Figure below represents MD models of GNP, GO and FGO:
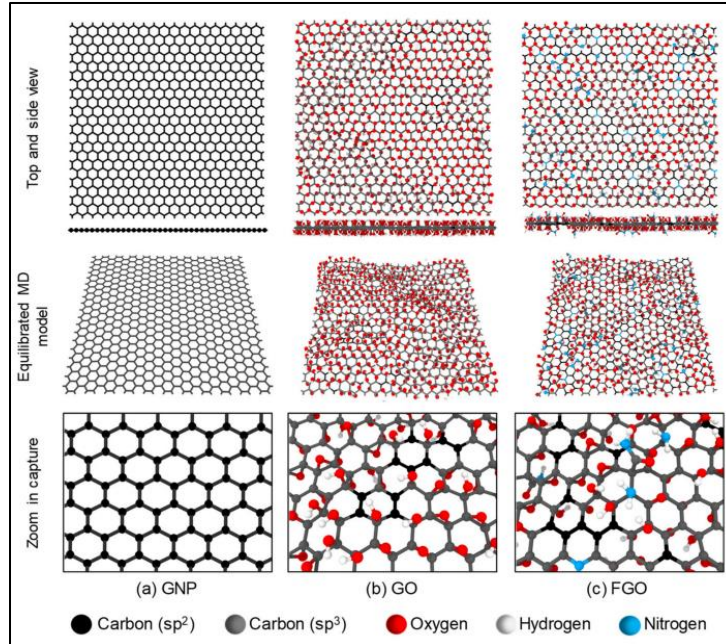
Figure 2.1 Representation of GNP, GO, FGO Nanoplatelets

The three nanoplatelet types were subjected to simulated uniaxial tensile deformations along the zigzag-axis to investigate the influence of functionalization on the structural integrity of graphene nanoplatelets. Figure-02 depicts the stress-strain responses of GNP, GO, and FGO. The GNP response clearly has the greatest elastic modulus of 1264 GPa. FGO and GO have moduli that are much smaller than 386 GPa and 119 GPa, respectively.

As a result, the nanoplatelet stiffness may be ordered according to their elastic moduli: GNP FGO > GO. The stiffer the graphene nanoplatelets, the lower the sp3/sp2 or functionalization degree. It concludes that presence of excessive functional groups degrades the stiffness of the functionalized graphene nanoplatelets.

13
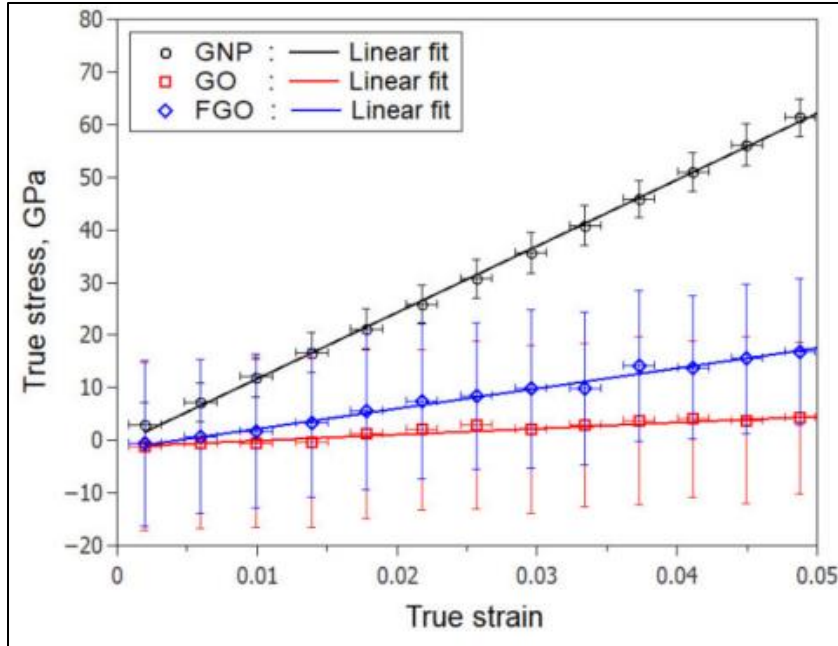
Figure 2.2 Stress-Strain response for GNP, GO and FGO Nanoplatelets

The effect of adding aluminum oxide, Al2O3, nanoparticles into Epocast 50-Al/946 epoxy glue at various temperatures when subjected to quasi-static tensile stress is statistically investigated (Hassan et al., 2022). ABAQUS/CAE has been employed to model a single-lap adhesive joint with two different types of material adherends (composite fiber-reinforced polymer (CFRP) and aluminum (Al) 5083 adherends) and the adhesive Epocast 50-A1/hardener 946. Four distinct adhesive regions i.e., middle plane of the adhesive location, middle longer edge along the length of the adhesive, shorter middle edge along the width of the adhesive and contact point of adherend and adhesive were used to investigate the effect of incorporating Al2O3 nano filler into the neat adhesive at three different temperatures of 25 °C, 50 °C, and 75 °C.

The inclusion of Al2O3 nanoparticles to the glue improved the epoxy's performance at elevated temperatures. The findings obtained revealed that the rise in peeling stress at the locations was more susceptible to tensile stresses at 50°C and 75°C temperatures compared to neat epoxy, imparting rigidity to the adhesive. When evaluating the joint perpendicular to the length dimension, it was revealed that the adhesive area of the SLJ experienced greater stresses toward the borders. Additionally, it was found that the central plane of the

adhesive location and the adhesive and aluminum adherend point of contact had been more susceptible to wear and tear initiation since the peak of stresses was near the boundary. This meant that the beginning of cracks would happen near the edges, which were extending the adhesive's length, and spread closer to the center, ultimately resulting in failure in life.

2.1 Factors Influencing CFRP and Al Adhesive bonds

Composite adhesive joints have been investigated by Ligang and Cheng under tensile loading. The study focused on changing geometry factors and examining the resulting behavior against tensile loading (Sun et al., 2019). The geometric factors included overlap lengths (7 specimen), adherend widths (5 specimens) and sequence of stacking of 3 specimen. 3D FEM model was utilized to analyze tensile behavior on single lap composite adhesive joint. This study concluded that changing the adherend width has more effect on the load carrying ability of the joint than changing overlap length. It was additionally thought that, in order to increase the joint's strength, the initial layer in the construction of CFRP substrate ought to be 0°. Based according to their research, cohesion failure is more common in SLJ with CFRP layering of [0/45 /-45 /90]3S, while delamination is more common in SLJ with CFRP layup of [90/-45/45/0]3S. Araújo and Machado (Araújo et al., 2017) examined the reaction of composite adhesive joints when subjected to impact loads. Ductile epoxy adhesive was employed to link two distinct material adherends. It was determined that these adhesives, in specific, and the combination of two distinct adherends, one of which is CFRP, demonstrate remarkable strength at impact and damping properties. Vibrational analysis was employed in their work to investigate damping capacities through dynamic testing.

Banea and Rosioara explored multi-material adhesive joints experimentally and statistically. Hard Steel (HS), Aluminum (Al), and CFRP, in the form of CFRP/Al and CFRP/HS, were utilized to produce adhesive joints (Banea et al., 2018). The influence of variables such as adherend stiffness and overlap length on the strength of composite adhesive joints was investigated. The findings revealed that the influence of material and/or

geometrical combination on joint strength is insignificant. Failure in SLJs with relatively short overlap lengths is primarily caused by global adhesive yielding.

Under tensile load, Campilho and Moura examined the residual stiffness and distribution of stresses of a refurbished composite plate (Campilho et al., 2005). Patch thickness, specimen design, and stack sequencing were essential characteristics for optimal performance. Various failure modes were explored mathematically, as well as the influence of layer characteristics on adhesive/adherend and patch/adhesive interfaces in those modes. Their findings revealed that adhesive strength has a significant impact on mode of failure, but interface and adhesive fracture toughness had minimal impact.

Wang and Liang looked at how the amount of loading affected the physical properties and failure mechanism of CFRP and Al alloy SLJ (Wang et al., 2020). Several rates of loading, notably 0.12, 4, 8, and 12 m/s, were employed for the shear test. Digital Image Correlation (DIC) was the technology used to examine the evolution of strains. According to their findings, the composite adhesive joint's shear strength rose as the loading rate increased. When the loading rate was raised from 0.12 m/s to 12 m/s, a substantially average rise in strength was seen, ranging from 19.3 MPa to 29.2 MPa. Fibre tear failure and cohesive failure were the two categories of failure that were noted.

The issue of adhesive delamination in composite adhesive single lap joints was examined by Morgado and Carbas (Morgado et al., 2020). By adding an adhesive layer to the adherends used in attachment, they investigated how to reduce delamination. The quasi-static loading and impact circumstances were the subject of an experimental examination. In quasistatic analysis, it was observed that delamination was prevented in addition to an increase in failure load. Wenlong and Guofeng looked at a joint that had aged hygrothermally (Mu et al., 2019). They concentrated their inquiry on the impact of varying loads on the joint's residual strength. The outcomes demonstrated that when the adhesive junction was subjected to hygro-thermal aging, its strength was severely weakened. The durability of the joints seems to deteriorate more quickly at greater loads when it is subjected to changing loading.

In their study, Monika and Jarosław compared the surface pretreatment and fiber arrangement in fiber metal laminates (FML). Glass was combined with aluminum and carbon fibers to create FML. Adhesive strength of the joint and cohesive failure was mostly determined by the kind of fiber utilized and the surface preparation applied to the adhesive junction (Ostapiuk et al., 2019). Comparative research on the shear strength of SLJs with various material adherends was conducted by Reis and Ferreira (Reis et al., 2011). Adherents made of composite, steel, and aluminum were combined in various ways. The primary factor affecting the joints' shear strength was adherent stiffness. The shear strength was also influenced by the overlap length in the adhesive joints, which varied according to the adherend material.

Experimental and numerical research was conducted by Ribeiro and Campilho on composite adhesive joints, or joints made of aluminum and carbon epoxy. The study took into account a variety of adhesive kinds as well as overlap length (Lo) (Ribeiro et al., 2016). The failure mechanism was explained by means of damage analysis and fracture development. The type of glue used has a significant impact on joint strength. When ductile glue was applied, the peak load (Pm) increased linearly, whereas brittle adhesive only exhibited very little improvement.

The impact of surroundings on the shear and tensile strength of the composite adhesive joints were examined by Jakub and Andrzej. CFRP and aluminum of a different grade—high strength and abrasion resistance—were combined to create composite joints (Korta et al., 2015). They also took into account two distinct kinds of adhesives during their analysis: adhesive for increased temperatures and adhesive for temperatures that are moderate. Humidity-temperature cycle tests were performed in accordance with SAE norms to access conditions. The findings demonstrated that, regardless of the absence of an external force, debonding of the epoxy occurs at humid and hot temperatures. Based on the quantitative research, the adhesive's thermal expansion coefficient was a significant element that significantly impacted the joints' performance under the given circumstances.

Research was done on dual adhesive in SLJ of various adherends by Jairaja and Narayana. It is well known that the kind and characteristics of the glue determine the strength of the

adhesive junction. They studied aluminum and CFRP composite adhesive joints, where it is more significant (Jairaja et al., 2019). They used Araldite 2015 and AV138 adhesives both alone and in mixture. They have combined the two types of glue; the brittle adhesive should be in the middle and the ductile adhesive should be at the ends. Their findings indicate that employing the two adhesives in the prescribed manner increased the durability of the composite adhesive joints.

2.2 Durability of adhesive joint under influence of temperature

Aluminum-aluminum adhesive junctions were studied for fracture properties at various low temperatures by Rahmani and Choupani. The findings demonstrated a rise in yielding strength, ultimate strength, and young's modulus at lower temperatures. It has been noted that when temperature decreases, rates of critical strain energy and stress factor concentration rise (Rahmani et al., 2019).

To be exact, Adamvalli measured the adhesive joint single lap's dynamic strength. Araldite® 2014 and titanium adherend made up the single lap joint (Adamvalli et al., 2008). The study was carried out at various loading rates and temperatures, ranging from 25 to 100 degrees Celsius. Dynamic loading was acting upon the single lap joint. Inspection of the joint showed that the adhesive layer was where the breakdown occurred. Furthermore, the study's findings demonstrated that, while strength considerably decreased at elevated temperatures, the rate of loading had the opposite effect.

The adhesive joints of CFRP/steel double-strap joints subjected to mechanical and thermal loads were examined by Nguyen and Bai. The ultimate load at room temperature—that is, 80%, 50%, and 20%—was the basis for loading levels. Additionally, the temperature was maintained between 35 and 50°C for every load level. Time-dependent behavior demonstrated the degradation of joint strength and stiffness with fn (time and temperature). Additionally, it was shown that recovery was stronger for cyclic thermal loading by around 47% compared to constant temperature loading (Nguyen et al., 2012).

Aluminum and CFRP composite adhesive joints were studied by Rahmani and Choupani. Their study's goal was to examine how the joint behaved at low temperatures, or between

-80°C and +22°C. After exposing the broken joints to temperature changes, tensile testing was done on the joint. To get a dimensionless stress intensity factor at low temperatures, a FEM was created. According to their findings, the variables might be enhanced by lowering the temperature to a certain point, beyond which the vital factors would drop (Rahmani et al., 2019). This ultimately resulted in the joint's ability to absorb fracture energy being reduced.

In their study, Ashcroft et al. (2001) examined double lap joints seen in jet aircraft. The joints underwent quasi-static and fatigue testing throughout a temperature variety. As adherends for adhesive connections, multi-directional MD and uni-directional UD CFRP were employed. To investigate the stresses in the adhesive composite joints, a numerical computation was carried out. The findings demonstrated that when temperature rose, joint strength and fatigue resistance both declined. Joints with UD CFRP adherends were sturdier at high temperatures in their research, while joints with MD CFRP adherends were stronger at cooler temperatures. According to their research, the pattern of activity they saw was caused by the adhesive joint's peak stresses controlling its strength at lower temperatures and creep in the joint controlling its strength at high temperatures, which is defined by the adhesive joint's minimum stresses. Finite element analysis provided evidence in favor of this claim.

Utilizing servo-hydraulic high-rate testing apparatus, Adamvalli and Parameswaran examined the impact of temperature change at increased dynamic loading on the strength of the SLJ joint. The findings, which illustrate joint failure and strength, were presented using the digital image correlation approach (Adamvalli et al., 2008). It was noted in the outcomes that shear strength and bond strength increased with loading rate. A rise in the average bond strength was seen when the temperature was changed from -25 to 50 degrees. Conversely, when the temperature varied from 50°C to 100°C, the joint's strength dropped (Adams et al., 1997). The findings of the inquiry also demonstrated the failure's conduct. The steel/adhesive interaction is thought to be the cause of the joint's failure at ambient temperature. It moved to the adhesive/BFRP interface at higher temperatures.

The research reviewed in this part leads to the conclusion that changing temperature parameters has an impact on the adhesive joint's or composite adhesive joint's effectiveness. It is evident from the available research that when temperature rises, the strength of a composite or simple adhesive bond generally decreases. The effects of lowering and raising temperatures are not the same. The body of research demonstrates the importance of the stress severity variables, which are ascertained using FEM. When the temperature is lowered further, these components first rise to the critical value before falling.

2.3 Composite Adhesive Bonds and Effect of Nanoparticles addition

An overview that emphasizes the advancement of nanoparticles in this field was given by Farid Taheri (Taheri et al., 2020). Particular attention should be placed on the works that address the use of nanoparticles to enhance the functionality of adhesive-bonded joints. Publications having a focus on FEM and a pertinent numerical analysis are taken into consideration. Scarselli and Corcione examined produced, tested, and simulated single lap joints. There were two kinds of adhesives used: one was regular adhesive, meaning it was connected with epoxy resin, and the other had both epoxy resin and nanographite granules. Dispersion graphene stacks that sonicated and expanded (EGS, 3%) in the epoxy matrix were made using the swelling technique (Scarselli et al., 2017). Their study demonstrates better mechanical qualities when epoxy is combined with nano-graphite. Quantitative characterization of adhesive performance with regard to durability and energy absorption makes this clear. Using CZM, the critical fracture energy and maximum shear stress were determined.

In order to enhance the effectiveness of adhesive-bonded joints in composite constructions, Khashaba used Epocast 50-A1/946 epoxy in combination with Multiwalled Carbon Nanotubes (MWCNTs). In a scarf adhesive joint SAJ, a 40% improvement over neat adhesive was noted (Khashaba et al., 2015). Additionally, a testing at a higher temperature was carried out, and the findings revealed a sharp decline in tensile strength. Water abortion also had an impact on tensile strength; a 2% loss was noted when compared to the dry sample.

In a different study, Khashaba examined the dynamic analysis of an adhesive junction under fatigue circumstances at different temperatures using a CFRP composite modified with aluminum oxide nanoparticles (Al2O3) (Khashaba et al., 2021). A hysteresis loop of stress-strain was employed to examine the dynamic variables, such as the damping factor, potential, and wasted energy Up. The scarf joint (SAJ) exhibited a 4.8% increase in shear strength at ambient temperature and a 24.5% rise at 50°C with the inclusion of nanoparticles, indicating positive outcomes. The fatigue strength decreased because to the lower glass transition temperature at 50°C.

Andrea and Alessandro looked into how aluminum nanoparticles affected epoxy strength. It was discovered that the addition of unprocessed alumina significantly extended fatigue life and shear strength. Shear strength enhanced by 60% statistically, and other attributes were also enhanced (Dorigato et al., 2011). It has been found that the mechanical characteristics of the adhesive were enhanced by the addition of alumina particles.

The impact of nanoparticles on the failure load associated with an adhesive joint was examined by Sunil and Dharmendra. The failure load was shown to rise when alumina nanoparticles were added to adhesive and utilized to create a single lap joint, according to empirical and computational analysis (Gupta et al., 2017). 23–47 nm alumina particles, which were produced using the polymerization process with 0.50 wt%, 1.00 wt%, 1.5 wt%, and 2.00 wt% of nanoparticles, were used to strengthen epoxy. Results showed that when nanoparticles were introduced to the junction, the failure stress increased in comparison to a neat adhesive joint. Out of all the examples, the shear strength of SLJ increased by more than 50% when 1.5% of alumina nanoparticles were present. In order to compare it with experimental analysis, 2D FEM modeling was built, and the results of the two investigations agreed. Finite element analysis was used to examine the peel, von-Mises, and shear stress distributions in order to determine the impact of reinforcement in the joint.

Khashaba looked at adding several kinds of nanoparticles to an epoxy adhesive. Comparing the effects of these infusions into the epoxy on the mechanical properties of the adhesive junction was the aim of this study. The MWCNTs, Al2O3, and SiC nanoparticles with varying weight percentages are ultrasonically disseminated into epoxy Epocast 50-A1/946

(Khashaba et al., 2014). In comparison to SiC and Al2O3 nanoparticles, the sonication duration and amplitude were lowered to prevent harming MWCNTs. Twelve clean nanocomposite joints were subjected to standard and plane shear testing. Whenever weighed against other weight proportions of nanoparticle materials, research has shown that MWCNTs (0.5wt.%), SiC (1.5wt.%), and Al2O3 (1.5wt.%) display better gains in attributes of tensile strength. Shear strength was increased by 5.5%, 4.9%, and 6.3%, respectively, with MWCNTs, SiC, and Al2O3. The shear moduli were enhanced by 10.3%, 16.0%, and 8.1%, accordingly, by MWCNTs, SiC, and Al2O3.

Salom and Prolongo looked at how the kind and amount of graphene nanoplatelets affected the thermo-mechanical characteristics and other parameters of the graphene epoxy nanocomposite. The modulus of elasticity of all nanocomposites was greater than that of pure epoxy thermoset resin. In the rubber state as opposed to the glass state, the storage modulus increased more (Salom et al., 2018). The aggregate of graphene nanoplates in the nanocomposites resulted in their fragility and lower tensile strength compared to pure epoxy thermoset resins. The nanocomposites of epoxy-GNPNH2 have a lower decreased fragility and tensile strength. Compared to pure epoxy adhesives, epoxy-graphene adhesives have a lower overlap shear strength. Lower lap shear strength was the result of higher CLT concentration. The functionalized and unfunctionalized forms of graphene are utilized. Functionalized graphene GNPNH2 included amine groups.

CHAPTER 3: METHODOLOGY

3.1 Finite Element Modeling:

Dassault Systems developed Abaqus CAE has been used as the Finite Element Modelling tool to perform design and simulation of the single lap joint for this study. A 2D model of the single lap joint, in which Aluminium 5052 was used as an adherend and cork powder filled Araldite LY-556 was an adhesive, was designed and simulated. There were two main components to the designing and simulation of the specimen:

•   Step-1: The initial step involved the 2D model designing of the single lap joint keeping the elastic properties of the adherend and adhesive in consideration.

•   Step-2: Simulation of the designed SLJ using different variations of the cork powder and temperature.

The focus of the research is such that two cases are built to make a fair comparison and hypothesis. First case was with the neat adhesive meaning that concentration of filler was at 0%. The second case was simulating the SLJ with mixture of epoxy and cork powder. In both the cases, different temperature variations e.g., 25C, 50C, 75C and 100C, were employed to examine the behavior of neat and filled adhesive.

3.1.1 Initial Geometry:

The geometry of the Single Lap Joint is shown in the figure below. The dimensions of the SLJ with adhesive and adherend were taken from the validation model. The adhesive is made of Araldite LY-556 and the adherend is made of Aluminium 5052. The adhesive is modelled as bi-directional material in which different layers of the adhesives are stacked perpendicular to each other that is 0o and 90o. The width of adherend Al-5052 is 25.4mm whereas its length is 101.6mm. The thickness of the adherend is 3mm. For the adhesive, Araldite LY-556, the length and width are 25.4mmx25.4mm whereas the thickness of the adhesive is 0.2mm.

In summarized words, the dimensions of the Al-5052 are 101.6 x 25 x 3. These dimensions have been taken from the validation model study focused on the experimentation of how cork particles can be used as a reinforcement material for fragile adhesives under varied temperature conditions. The dimensions of adhesive region, as taken from the research above, are 25.4 x 25.4 x 0.2.
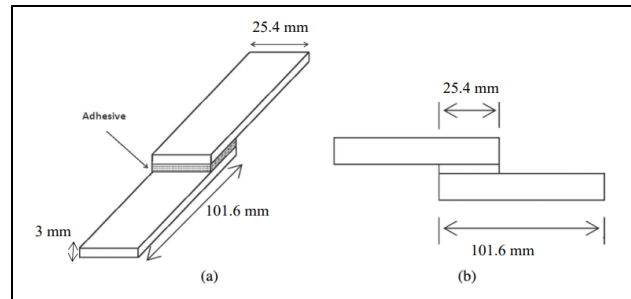
Figure 3.1 Dimensions of Single Lap Joint

The material model that has been used for the Aluminium and araldite adhesive and adherend was elastic. It means that the behavior of stress strain for the given material was considered to be elastic only. This elastic behavior was examined at different temperature variations such as 25oC, 50oC, 75oC and 100oC. The material properties of adherend and adhesive are listed in the tables below:

Table 3.1 Properties of Adherend

Material Property	Aluminium 5052
Young's Modulus (GPa)	70.3
Poisson Ratio (v)	0.33
Yield Strength (MPa)	193
Ultimate Strength (MPa)	228
Shear Strength (MPa)	138

Table 3.2 Properties of Adhesive

Material Property	Araldite LY-556
Aspect (Visual)	Clear Liquid
Viscosity at 25°C (ISO-12058-1)	10000 – 12000 (mPa s)
Density at 25°C (ISO-1675)	1.15 – 1.2 (g/cm^3)
Epoxies' index (ISO 3001)	5.30 – 5.45 ** (Eq/Kg)

Table 3.3 Properties of Hardener

Material Property	Hardener (AD-22962)
Aspect (Visual)	Colorless-little yellow liquid
Viscosity at 25°C (ISO-12058-1)	5 - 20 (mPa s)
Density at 25°C (ISO-1675)	0.89 – 0.90 (g/cm^3)

Aluminium AL-5052's composition is extremely lightweight, and it has excellent strength against fatigue, strong resistance to corrosion, and better weldability. Al 5052 is therefore incredibly helpful when used in heat exchangers, chemical storage, fuel tanks, pressure vessels, oil lines, and other applications.

In these trials, cork powder has been utilized as a filler. Advantages of cork include:

•   Its elasticity makes it an excellent material for fracture barriers due to its highly impervious nature.

•   Stretching or compressing cork does not significantly change its radius because of its almost negligible Poisson's ratio.

•   Cork may be described as a homogeneous tissue with consistently coordinated, thin-walled cells that lack intercellular gaps. Cork has an alveolar structure that resembles a honeycomb, with no spaces between consecutive cells and closed units. The composite can withstand greater impact thanks to this cell structure than it could with brittle resin without particles.

3.1.2 Boundary and Loading Conditions:

The loading and boundary conditions for the simulation of single lap joint under application of Finite Element Analysis (FEM) is shown in figure 3.2 below. Two different types of boundary conditions have been used on the joint. The joint is fixed from one end and is restricted for motion in y and z axis on the other side. One was encastre boundary condition fixing the left edge of the adherend. Tensile loading using displacement loading of 0.3mm was applied to the right side of the adherend. The single lap joint has only been allowed one degree of freedom that is in x-direction (with the help of roller support). Y-direction movement of the SLJ has been fixed to avoid any vertical motion. A tie constraint was used between contact surfaces of adhesive and adherend. SLJ has been subjected to a force of 6000N in the direction of one body of freedom (x-axis).
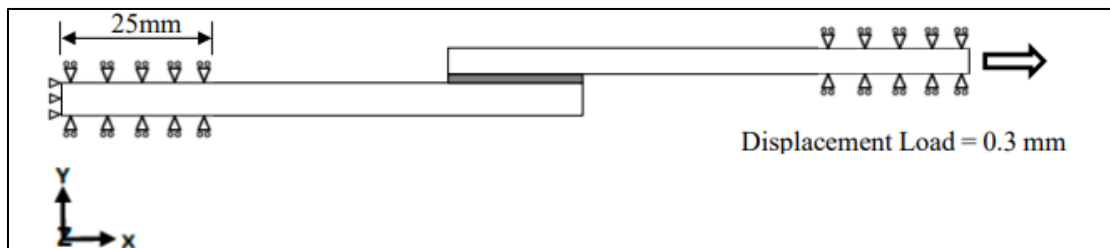
Figure 3.2: Boundary and Loading Conditions of Single Lap Joint (SLJ) (Not to Scale)

3.1.3 Mesh Element Generation Methodology:

Implementing mesh in single lap joints with eccentric loads requires careful consideration of the bending of the SLJ under tensile stress. If the mesh has the ability to accurately depict both the distorted and undeformed shape of the SLJ, it may be deemed to be well-meshed.

There are two main approaches that may be used to mesh an adhesive joint. The first technique involves creating a changeable mesh that, at a specific location of interest, transitions from coarse to fine mesh. With this approach, the SLJ is divided or partitioned into many areas, enabling the provision of variable-sized seeds along the boundaries of the regions and the ability to seed each region independently. The second technique applies the mesh to each component independently. This implies that the sections that are not of interest can have mesh that is rather coarse, while the region of significance can have fine mesh, similar to the adhesive. As a result, detailed (fine) mesh is required in the adhesive

26

and coarse mesh is possible to be put on the adherends. Pre-processing is more time-consuming in the first way than in the second since the model or portion of it is divided into sections that can seed independently of one another. The second strategy is implemented to the SLJ sections in this study. The second approach was used since the adherend only required one component in the direction in which the piles were stacked.

Structured mesh was used to mesh all the parts of the SLJ. This method employs pre-defined pattern and shape of elements unlike the free mesh method. The adherend is given structured mesh with twelve elements along the thickness while the adhesive has been given eight elements along the thickness. Figure 3.3 shows the structured mesh in form of rectangular elements for all parts of the single lap joint.

The global mesh size for the adherend is 3mm. Whereas, local seeding method was used for the adhesive containing eight elements along the thickness. Uniform sizing of the elements has been kept as priority during mesh generation of SLJ. Approximately, 150 elements on each edge of the adhesive have been assigned. The total number of elements in the single lap joint are ~12,000.

A mesh convergence study was conducted before the single lap joint's meshing was finalized. Meshes of 0.25×0.06 mm, 0.125×0.03 mm, 0.05×0.03 mm, 0.025×0.03 mm, and 0.05×0.0124 mm were included in the mesh convergence investigation. The mesh convergence criterion was based on stresses in the adhesive layer. The finished mesh had eight pieces with a thickness of 0.05×0.03 mm in the adhesive layer. A finer mesh was employed in the adherends close to the overlap zone, while a coarser mesh was utilized in the sections farther from the overlap region, in addition to this overall mesh size. In order to do this, biased seeds were used to create the mesh along the adherends' length.

3.1.4 Type of Mesh Element:

Mesh element type was considered based on the tensile loading response for the single lap adhesive joint. Due to eccentricity of the load applied the single lap joint faces bending when tensile load is applied on it. Linear 4-node brick element with reduced integration (CPE4R) was used for adherend and adhesive regions. A linear-explicit model for type of

mesh element has been selected with hourglass control because for linear static analysis in ABAQUS, the "linear-standard" element type is frequently utilized. While dealing with this kind of element (and comparable sorts), hourglass control methods are crucial for preventing or managing hourglass deformations.

An hourglass mode in finite element analysis is an unphysical, parasitic mode of deformation that can arise in some element types when there is insufficient stiffness or when the analysis is not well-constrained. Numerical instability and erroneous findings are possible outcomes. Numerous methods and measures can be used to lessen hourglassing. Using constraint algorithms or specific components intended to reduce hourglassing are common techniques.

In engineering and structural analysis, linear static analysis is a fundamental method used in Finite Element Analysis (FEA) to forecast the behavior of structures and its constituent parts under different loads and forces. It is suitable when material characteristics stay constant during the study and deformations are deemed modest since it functions under the assumptions of linear material behavior and small deformations. Solving the equilibrium equations is the fundamental task of linear static analysis, which verifies that the total of the forces and moments acting on the structure is balanced. One of the most important preconditions for a successful analysis is having well stated boundary conditions, which indicate how the structure is supported or restricted. Accuracy depends on proper meshing, or the breaking down of the geometry into smaller components. The resultant system of linear equations is then numerically solved by the FEA program utilizing methods like the stiffness matrix and load vector. The information gathered includes displacements, stresses, strains, and reaction forces—all essential for determining if the structure satisfies design specifications.

Figure 3.4 shows the meshing of each part of the single lap joint from adherend to the adhesive.
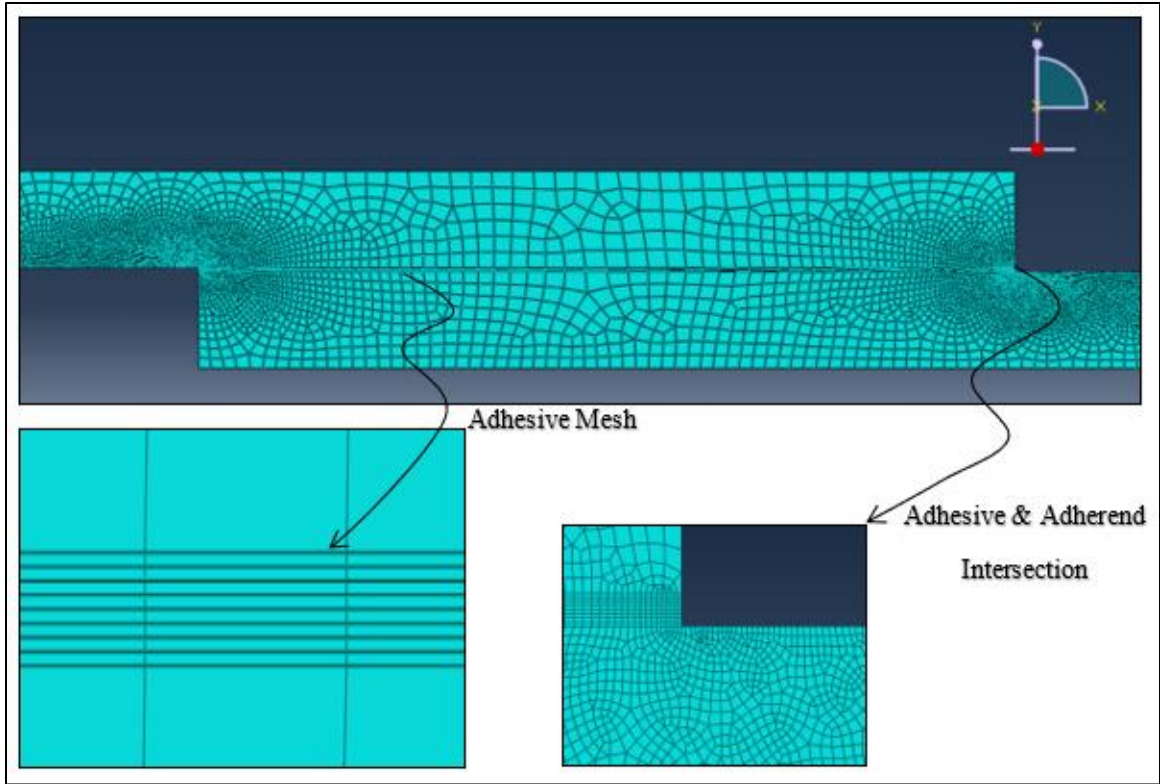
**Figure 3.3: Single Lap Joint (SLJ) all parts mesh**
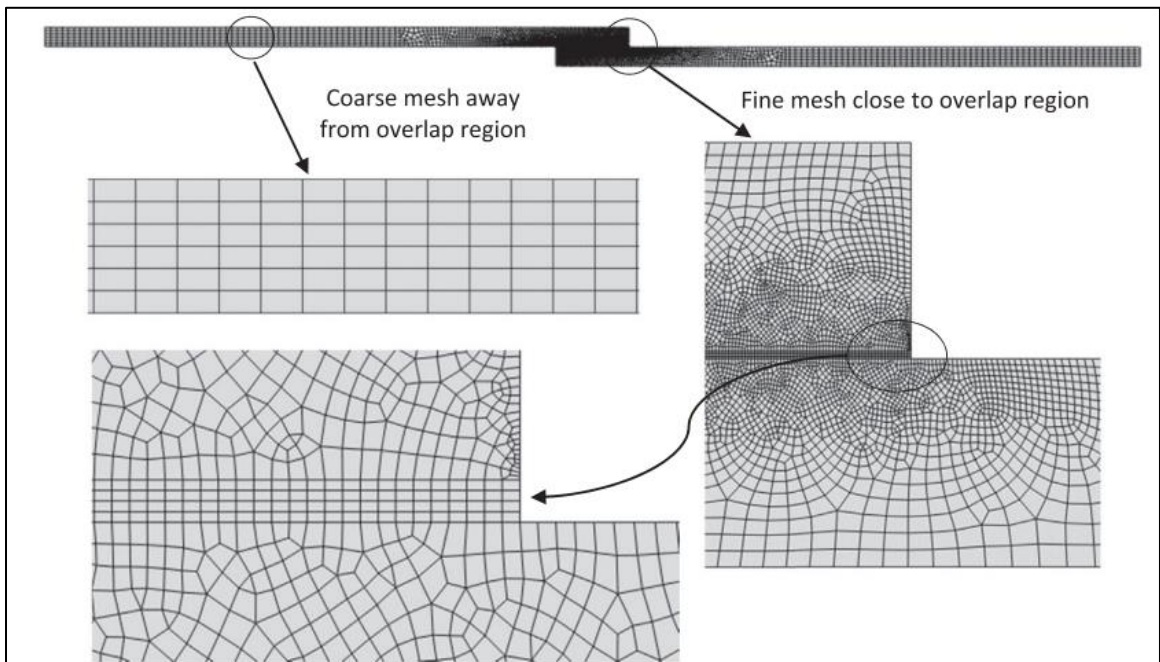
**Figure 3.4: Adhesive and Adherend detailed mesh**

3.1.5 Finite Element Model Validation:

Topology optimization of adhesive joints using non-parametric methods research was used as a reference model for this research. To validate the design first of all a validation model was prepared, results of which were compared with that of the reference model. Taking the concept of 2D stress analysis from that work, the methodology was implemented in the current work. Peel and shear stress analysis was performed for current model and graphs were compared with that of reference study.
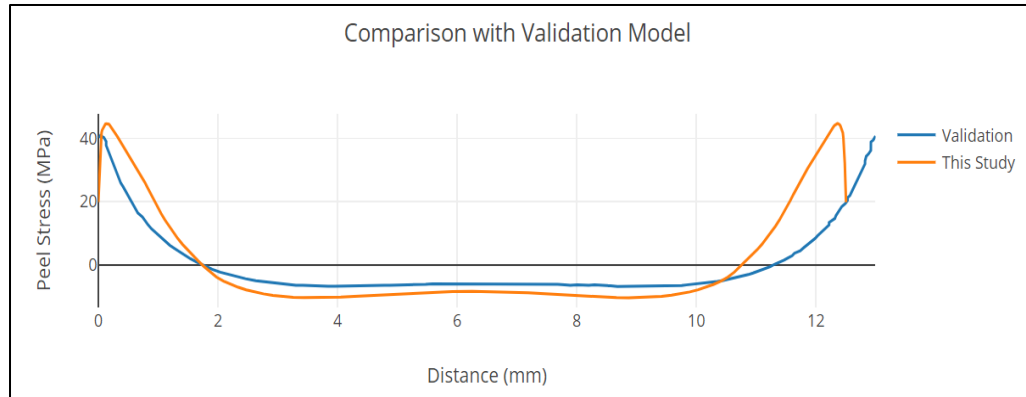
Below, figure 3.5, is the geometry of the reference/validation model that was initially designed and analysis was performed on. The results were then compared which are shown in figure 3.6.
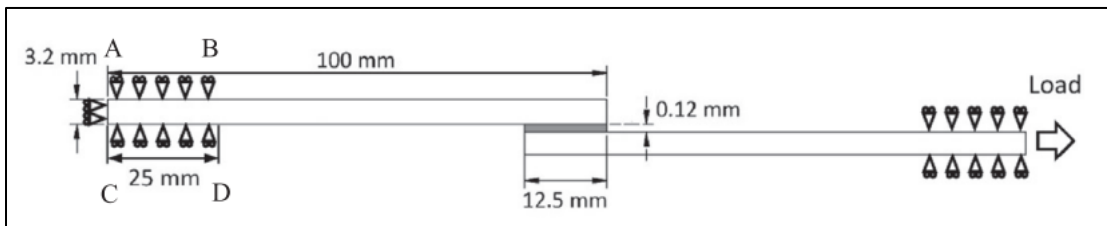
Figure 3.5: Single Lap Joint Geometry of the Validation model
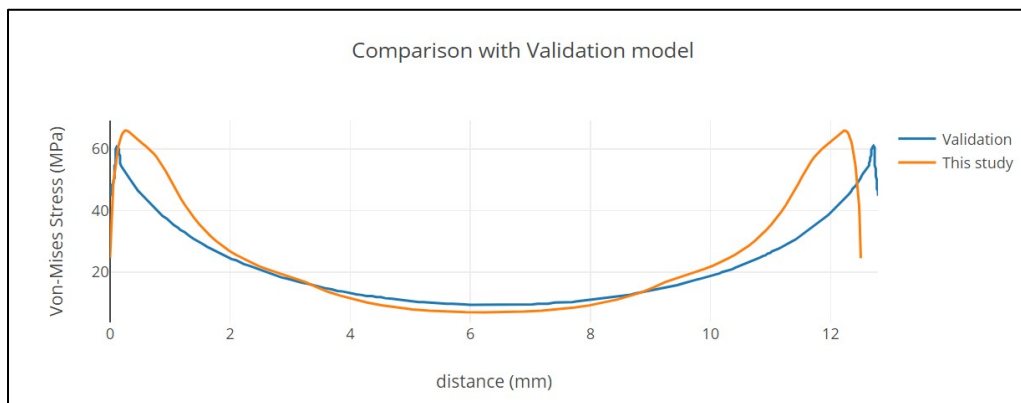
Figure 3.6: Comparison of Von-Mises Stress in the middle of adhesive layer of SLJ between reference and current study

Figure 3.7: Comparison of Peel Stress in the middle of adhesive layer of SLJ between reference and current study

The reference work displays peel stress at the adhesive's edge same as the current study demonstrates higher peel stress at the edges of the adhesive. Furthermore, the pattern in this phenomenon is the same, indicating that when examining a single lap joint, the ends experience large loads and are more prone to failure.

CHAPTER 4: RESULTS AND DISCUSSION

This chapter discuss the results of the current research and simulation study with the help of graphical data that has been obtained by the Finite Element Method (FEM) analysis performed on the 2D single lap joint. Focus of this research are the following cases:

1)   Neat adhesive single lap joint that is pure LY-556/Hardener AD-22962

2)   Adhesive with cork powder nanoparticles added

Single lap joint in both cases has been subjected to different temperatures including 25ºC, 50ºC, 75ºC and 100ºC. The effect of nano fillers on the SLJ at geometric locations is the prime objective of this study. Peel and shear stress are the main stresses that this study is focusing on, which occur in the adhesive layer during load application at the middle of the long edge face (along the length of adhesive). Path has been drawn at this location to get the necessary data. The cases have been separately discussed in the sub sections followed by a comparative study.

4.1 Neat Adhesive Layer:

Neat adhesive case of the single lap joint was subjected to tensile loading by applying displacement of 0.3mm. The single lap joint is facing bending caused by tensile loading that leads to peel and shear stress. The peel and shear stress in this research are examined at the middle of the adhesive layer. Single lap joint has been analyzed at four different temperatures at neat adhesive configuration. These temperatures are 25ºC, 50ºC, 75ºC and 100ºC. following section discusses the peel and shear stress distribution over the overlap region at the middle of the adhesive layer.

The path at the middle plane of the adhesive is shown in the figure 4.3 below. It can be noted that the peak peel loads are: 81.58 MPa, 57.63 MPa, 49.01 MPa and 41.27 MPa at temperatures of 25ºC, 50ºC, 75ºC and 100ºC respectively. Increasing temperature from 25ºC to 50ºC results in a 29.35% decrease in peel stress. Similarly, increasing temperature further from 50ºC to 75ºC decreases the peel stress about 39.92% from initial reading.

Consequently, at temperature of 100ºC, the peel stress decreases 49.41% from the actual value at 25ºC.

As far as shear stress is concerned, the peak values at temperatures of 25ºC, 50ºC, 75ºC and 100ºC are 46.52 MPa, 33.71 MPa, 28.92 MPa and 24.55 MPa, respectively. It means that from 25ºC to 50ºC the drop in shear stress is 27.53%, from 50ºC to 75ºC it is 37.83% and at temperature of 100ºC it has dropped by 47.22%.

Peel stress shows greater variation along the length and eventually drops to zero. The graph can be seen to go down below zero which indicates the presence of compressive stress. For adhesive, the variation at 25ºC is high compared to at increased temperatures. This is because of drop of stiffness and elastic modulus of adhesive at increased temperatures. Figure below shows high peel stress at edges of the adhesive layer because of bending moment. Crack initiation in the adhesive-adherend interface will most likely start from the edges if the joint failure is considered.

Shear stress caused by the tensile loading plays a definitive role in determining the strength of the adhesive joint. On increasing temperature, the shear stress is consequently reducing meaning that the strength of the adhesive joint in terms of its resistance to breakage is decreasing.

Figure 4.1 and 4.2 show the peel and shear stress graphs of the single lap joint middle adhesive layer:
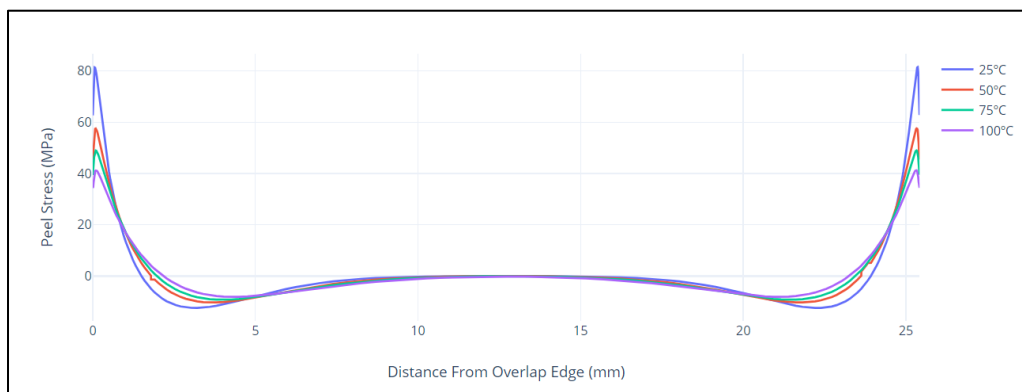
Figure 4.1: Peel Stress at various Temperatures (Mpa)
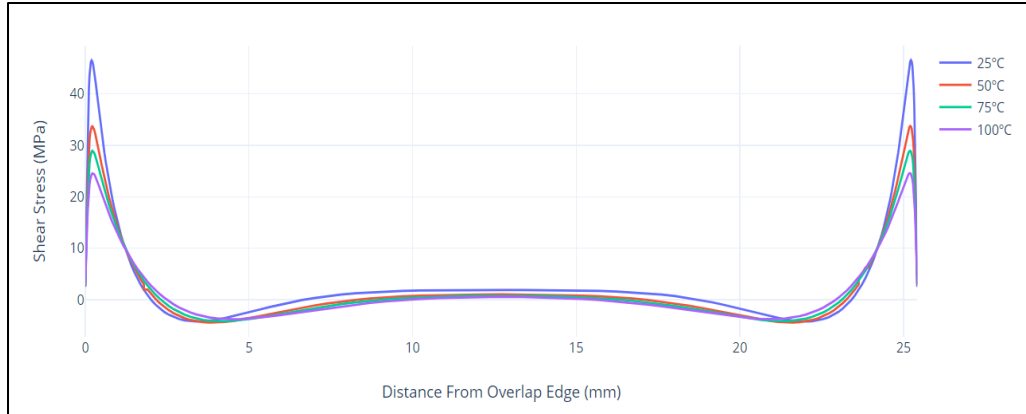
Figure 4.2: Shear Stress at various Temperatures (Mpa)

Figure 4.2 makes it clear that, given the structure of the joint, the failure is most likely to begin at the location approximately 0.7 mm inward of the edge of the joint. Peel stress is more important in the beginning of the joint fracture. Because of this, it's crucial to understand this tension. As you can see in figure 4.2, the fracture will start from both joint borders and move toward the adhesive core. Compared to 50°C and 75°C, peel stress is higher at 25°C. The resistance to the change in deformation in tensile loading is the more likely cause.

Figure 4.3 shows the middle plane of the adhesive layer on which the FEA analysis for the neat adhesive layer has been performed:
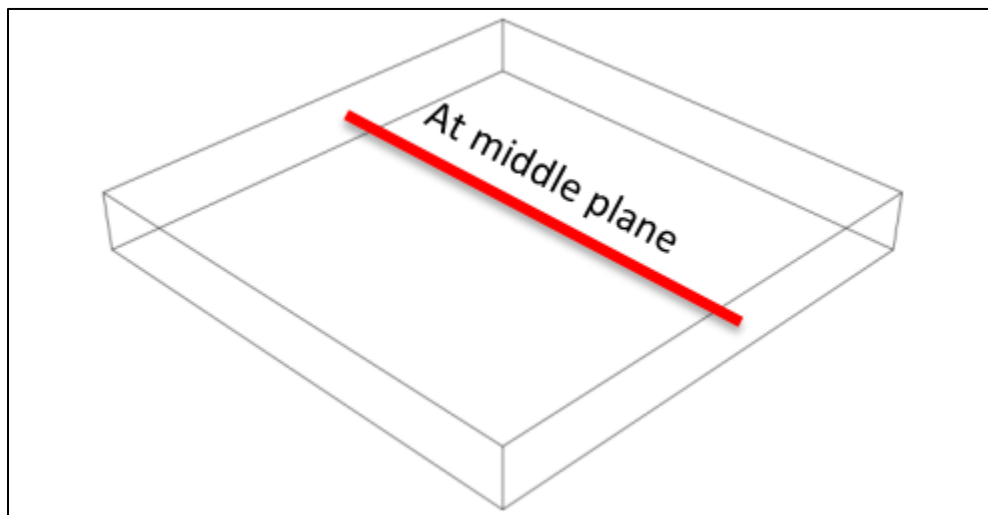
Figure 4.3: Path at middle plane of adhesive layer for Peel and Shear Stress

4.2 Adhesive with 25wt% of Cork Powder:

For nano particle addition cork powder was selected. Adhesive with 25wt% of cork powder was subjected to FEA analysis by tensile loading application at a displacement of 0.3mm. The single lap joint is facing bending caused by tensile loading that leads to peel and shear stress. The peel and shear stress in this research are examined at the middle of the adhesive layer. Single lap joint has been analyzed at four different temperatures at 25wt% of cork powder in adhesive. These temperatures are 25ºC, 50ºC, 75ºC and 100ºC. following section discusses the peel and shear stress distribution over the overlap region at the middle of the adhesive layer.

It can be noted that the peak peel loads are: 79.41 MPa, 56.48 MPa, 52.76 MPa and 40.96 MPa at temperatures of 25ºC, 50ºC, 75ºC and 100ºC respectively. Increasing temperature from 25ºC to 50ºC results in a 28.87% decrease in peel stress. Similarly, increasing temperature further from 50ºC to 75ºC decreases the peel stress about 33.56% from initial reading. Consequently, at temperature of 100ºC, the peel stress decreases 48.41% from the actual value at 25ºC.

As far as shear stress is concerned, the peak values at temperatures of 25ºC, 50ºC, 75ºC and 100ºC are 45.44 MPa, 33.07 MPa, 31.01 MPa and 24.37 MPa, respectively. It means that from 25ºC to 50ºC the drop in shear stress is 27.22%, from 50ºC to 75ºC it is 31.75% and at temperature of 100ºC it has dropped by 46.36%.

Peel stress shows greater variation along the length and eventually drops to zero. The graph can be seen to go down below zero which indicates the presence of compressive stress. For adhesive, the variation at 25ºC is high compared to increased temperatures of 50ºC, 75ºC and 100ºC. This is because of drop of stiffness and elastic modulus of adhesive at increased temperatures. Figure below shows high peel stress at edges of the adhesive layer because of bending moment. Crack initiation in the adhesive-adherend interface will most likely start from the edges if the joint failure is considered.

Shear stress caused by the tensile loading plays a definitive role in determining the strength of the adhesive joint. On increasing temperature, the shear stress is consequently reducing
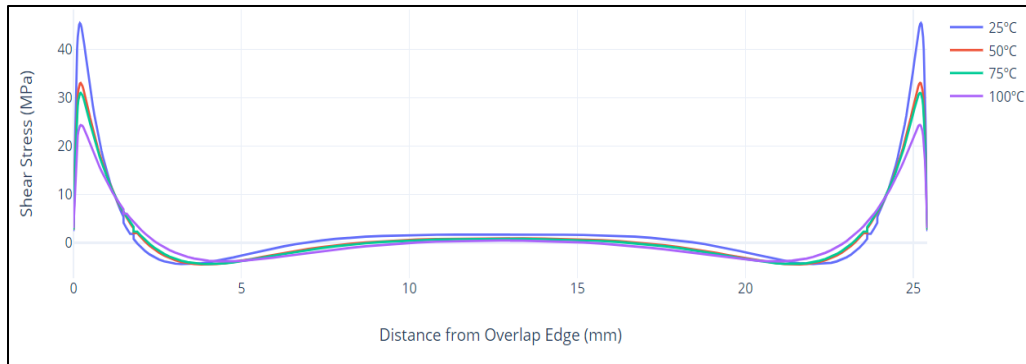
meaning that the strength of the adhesive joint in terms of its resistance to breakage is decreasing.

Figure 4.4 and 4.5 show the peel and shear stress graphs of the single lap joint middle adhesive layer:
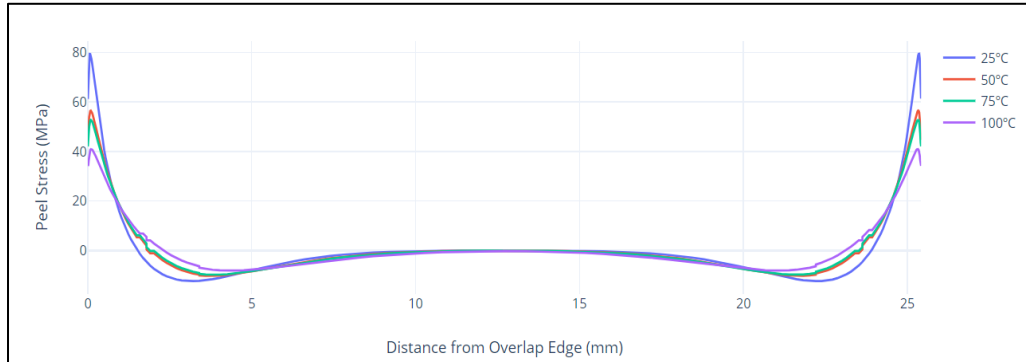
Figure 4.4: Peel Stress at various Temperatures (Mpa)

Figure 4.5: Shear Stress at various Temperatures (Mpa)

4.3 Adhesive with 50wt% of Cork Powder:

Adhesive with 50wt% of cork powder was subjected to FEA analysis by tensile loading application at a displacement of 0.3mm. The single lap joint is facing bending caused by tensile loading that leads to peel and shear stress. The peel and shear stress in this research are examined at the middle of the adhesive layer. Single lap joint has been analyzed at four different temperatures at 50wt% of cork powder in adhesive. These temperatures are 25ºC,

50ºC, 75ºC and 100ºC. following section discusses the peel and shear stress distribution over the overlap region at the middle of the adhesive layer.

It can be noted that the peak peel loads are: 68.42 MPa, 56.53 MPa, 51.97 MPa and 42.77 MPa at temperatures of 25ºC, 50ºC, 75ºC and 100ºC respectively. Increasing temperature from 25ºC to 50ºC results in a 17.37% decrease in peel stress. Similarly, increasing temperature further from 50ºC to 75ºC decreases the peel stress about 24.04% from initial reading. Consequently, at temperature of 100ºC, the peel stress decreases 37.48% from the actual value at 25ºC. It can be noted that although the peek stresses at each temperature are lower than peak stresses of respective temperatures at 25wt%, the variation of peek stresses across different temperatures is lower in 50wt% than in 25wt%. It symbolizes that at a weight percentage of 50 can result in stable peel stress peaks at various temperatures instead of a gradual decent.

As far as shear stress is concerned, the peak values at temperatures of 25ºC, 50ºC, 75ºC and 100ºC are 39.54 MPa, 33.10 MPa, 30.57 MPa and 25.41 MPa, respectively. It means that from 25ºC to 50ºC the drop in shear stress is 16.28%, from 50ºC to 75ºC it is 22.68% and at temperature of 100ºC it has dropped by 35.73%. Results of shear stress are almost similar for 25 and 50wt% at temperatures of 50ºC and 75ºC hence, they can be considered as ideal temperature and weight percentages for addition of cork powder in adhesive.

Peel stress gradually decreases to zero and varies more throughout its length. It is evident that the graph descends below zero, signifying the existence of stress caused by compression. Comparing higher temperatures of 50, 75, and 100°C to adhesive, the variance is greater at 25° Celsius. This is caused by the adhesive's modulus of elasticity and hardness decreasing at higher temperatures. The bending moment causes considerable peel stress at the adhesive layer's edges, as seen in the figure following. If the joint failure is taken into account, crack propagation at the interface of adhesive and bonding plates will most likely begin from the outer edges.

Figure 4.6 and 4.7 show the peel and shear stress graphs of the single lap joint middle adhesive layer:
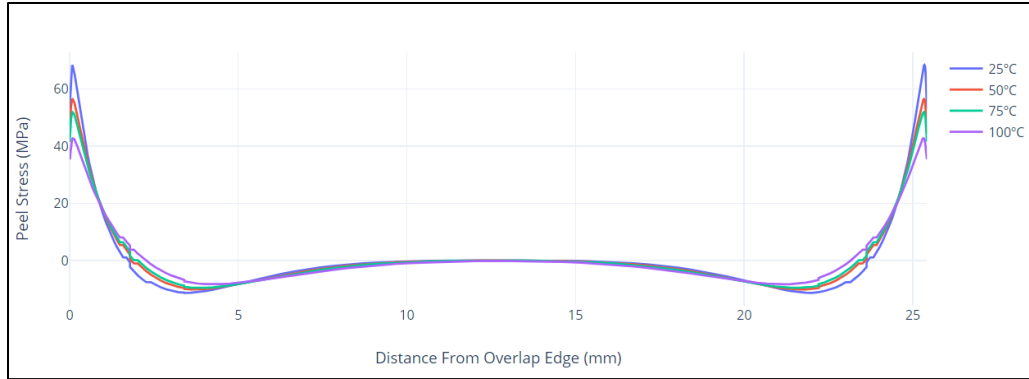
Figure 4.6: Peel Stress at various Temperatures (Mpa)
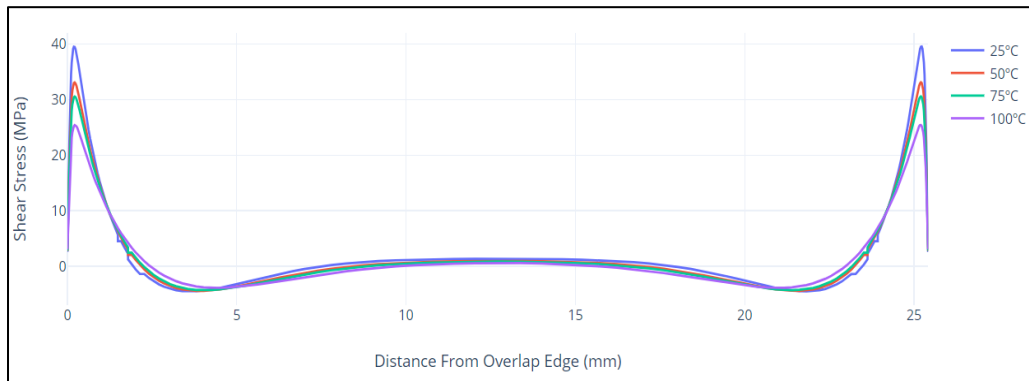
Figure 4.7: Shear Stress at various Temperatures (Mpa)

It is evident from Figure 4.6 that the failure is most likely to start at a point around 0.6-0.7 mm inward of the joint edge due to the nature of the joint. When a joint fracture first occurs, peel stress is more significant. It's vital to comprehend this tension as a result. The fracture will begin at either of the joint borders and progress in the direction of the adhesive core, as shown in figure 4.6 peel stress is greater at 25°C than it is at 50°C and 75°C. The most likely cause is resistance to the change in deformation in tensile stress.

4.4 Adhesive with 75wt% of Cork Powder:

After 50wt%, an addition of more cork powder was made leading to a 75wt% adhesive for adherend bonding layers. Middle of the adhesive layer has been taken for FEA analysis. Peel and shear stress show their peaks at the edges of the adhesive hence it can be said that crack initiation happens at the edges. Both the stresses approach to zero and below zero at

the center of the adhesive. With increase in temperature the strength and bonding qualities of the adhesive gradually fall which indicates a decreased modulus of elasticity.

Peak values for peel stress for a weight percentage of 75% at four different temperatures of 25ºC, 50ºC, 75ºC and 100ºC are 61.27MPa, 52.96MPa, 52.90MPa and 43.06MPa, respectively. From 25ºC to 100ºC the peel stress dropped by a percentage of 29.72%. Likewise, the peak values of shear stress at 25ºC, 50ºC, 75ºC and 100ºC are 35.71MPa, 31.12MPa, 31.09MPa and 25.58MPa. From 25ºC to 100ºC the shear stresses drop by a percentage of 28.36%.

Figure 4.8 and 4.9 show the peel and shear stress graphs of the single lap joint middle adhesive layer:
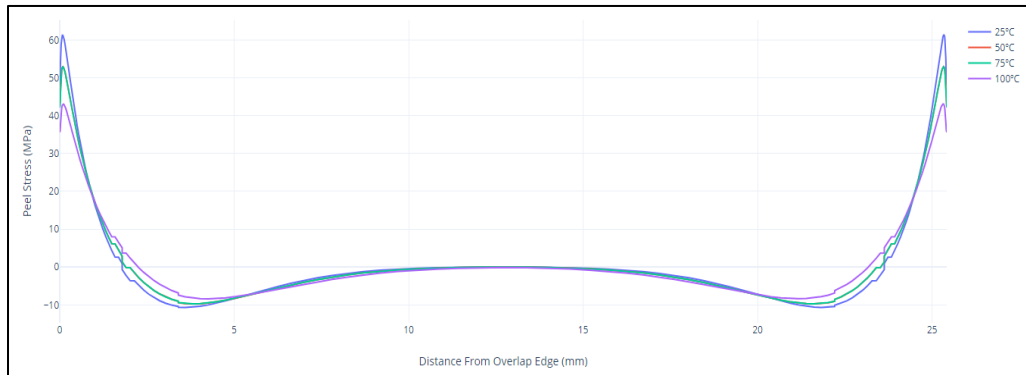
Figure 4.8: Peel Stress at various Temperatures (Mpa)
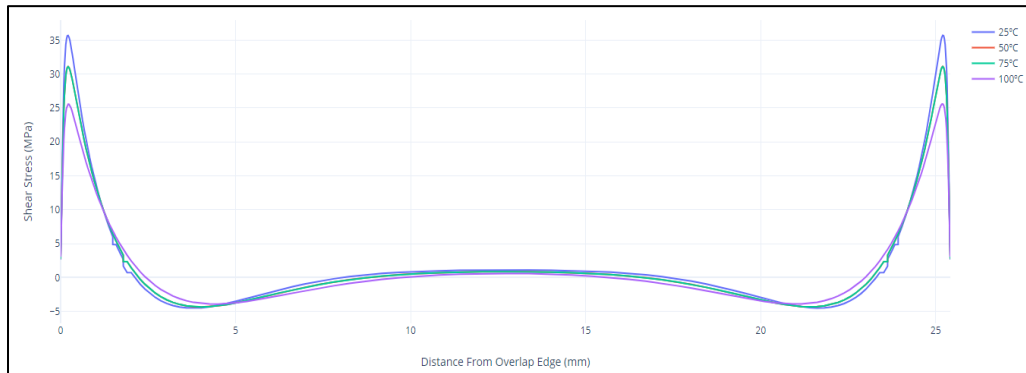
Figure 4.9: Shear Stress at various Temperatures (Mpa)

At higher temperatures, several adhesives display thermal softening or a decrease in viscosity. This may result in a drop in the shear stress and, in turn, a decrease in the shear modulus. The adhesive's molecular mobility may increase with temperature, making it more malleable and less resistant to deformation. Elevated temperatures have the potential to speed up adhesive deterioration or impair the adhesive-substrate contact. Shear stress may diminish as a result of early debonding and failure brought on by this.

4.5 Adhesive with 100wt% of Cork Powder:

Crack initiation at the edges of the adhesive layer is a notable parameter of this research. Shear stress propagated crack initiation refers to fracture formation inside the adhesive layer parallel to the interface of adherend. This type of fracture failure is linked to sliding or displacement along the plane of adhesion, leading to localized concentration of stress. On the other hand, peel stress induced crack initiation involves separation or peeling of adherends at the adhesive contact. The ripping or separating load tends to apply on the adherends causing tensile strain at the interface. The concentration of these tensile stresses, particularly at the adhesive edges, might exceed the adhesive material's cohesive strength, causing fractures to form and propagate along the interface.

At about 0.7mm overlap distance, the peak values of peel and shear stress are observed that means that the crack initiation happens at the edges of the adhesive. at the center of the interface, the stresses drop to zero or below zero meaning a decreased elastic modulus.

Peak values for peal stress for a weight percentage of 100% at four different temperatures of 25ºC, 50ºC, 75ºC and 100ºC are 69.43MPa, 51.73MPa, 53.85MPa and 46.02MPa, respectively. From 25ºC to 100ºC the peel stress dropped by a percentage of 33.71%. Likewise, the peak values of shear stress at 25ºC, 50ºC, 75ºC and 100ºC are 40.08MPa, 30.44MPa, 31.61MPa and 27.24MPa. From 25ºC to 100ºC the shear stresses drop by a percentage of 32.03%.

Figure 4.10 and 4.11 show the peel and shear stress graphs of the single lap joint middle adhesive layer:
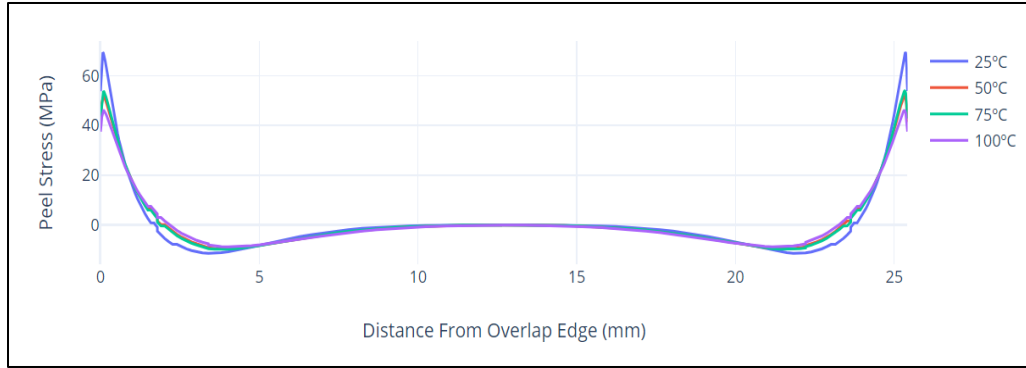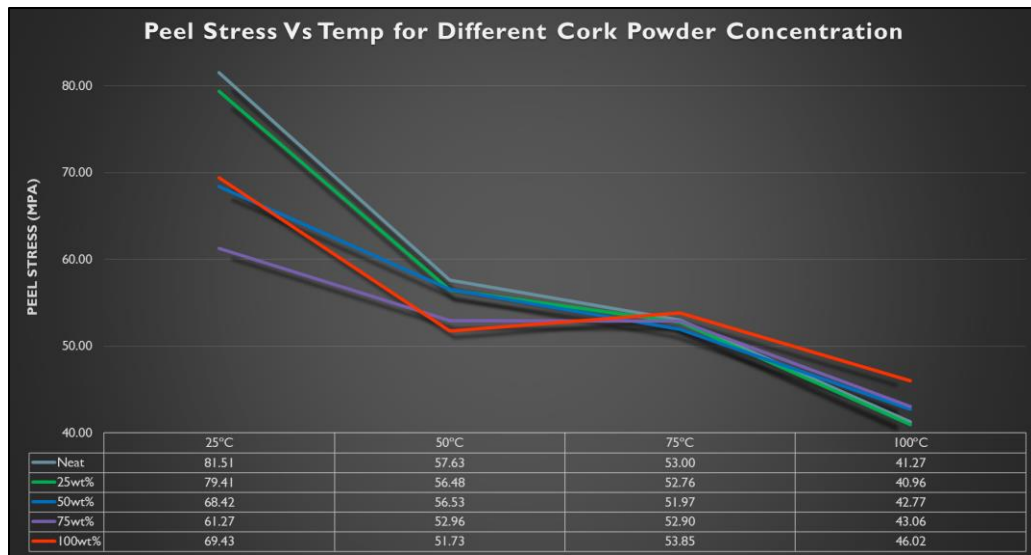
Figure 4.10: Peel Stress at various Temperatures (Mpa)
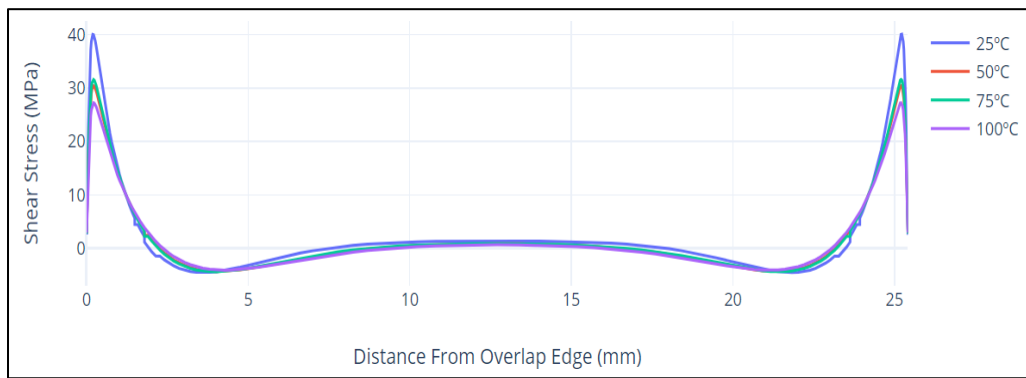
**Figure 4.11: Shear Stress at various Temperatures (Mpa)**

4.6 Comparison between Neat and filler induced Adhesive:

Below charts show a comparison between peel and shear stress at neat adhesive and filler induced adhesive for different cork powder concentrations:

Graph 4.1: Graphical depiction of Peel stress at all concentrations of cork powder

Generally, a decrease in peel stress is observed as the temperature increases, regardless of the cork powder concentration.
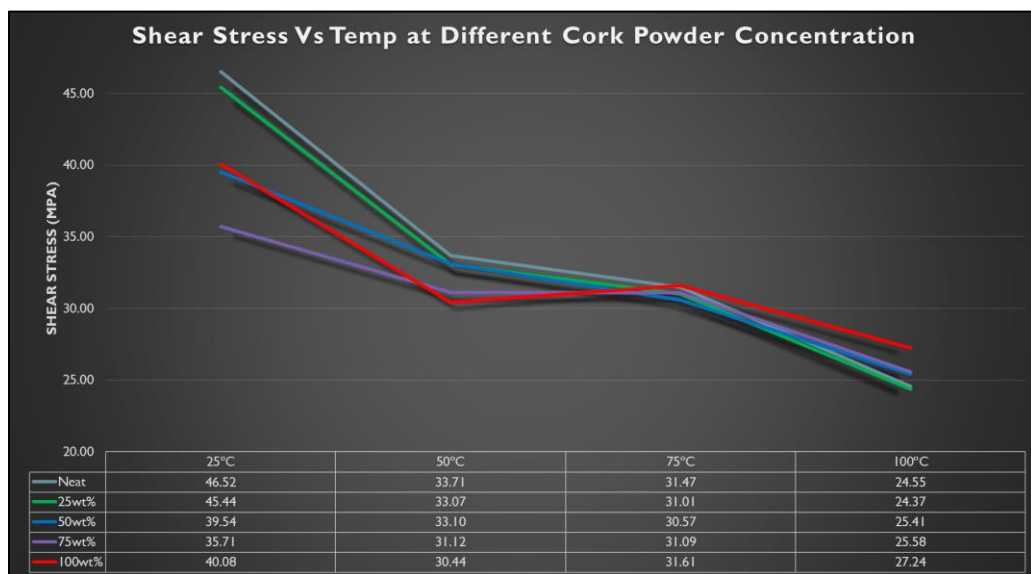

Graph 4.2: Graphical depiction of Shear stress at all concentrations of cork powder

Similar to peel stress, shear stress tends to decrease with increasing temperature across all concentrations of cork powder.

The phenomenon of decreasing peel and shear stress can be explained by theory of material softening in which at elevated temperatures the adhesive tend to become for ductile and soft. It means that the material is more likely to deform rather than fracture as is explained in literature review (Adams et al., 1997). At all weight percentages the value of peel and shear stress decreases meaning that at same concentration the failure strength decreases by increasing the temperature. Moreover, with increase in temperature the distribution and dispersion of cork powder enhances within the material. This improved homogeneity results in a more uniform stress distribution that reduces the localized stress concentration. Crack initiation in the adhesive layer has been observed at the edges of adhesive due to reduction in modulus of elasticity and mismatch between the adhesive and adherend material.

Following figures from Abaqus CAE depict the FEM model of the single lap adhesive joint with stress and strain profiles. It can be seen that more stress concentration is observed on the edges of the adhesive and adherend interface due to peel stress and comparatively lower stress is observed in the adherend elsewhere.

(a)

(b)
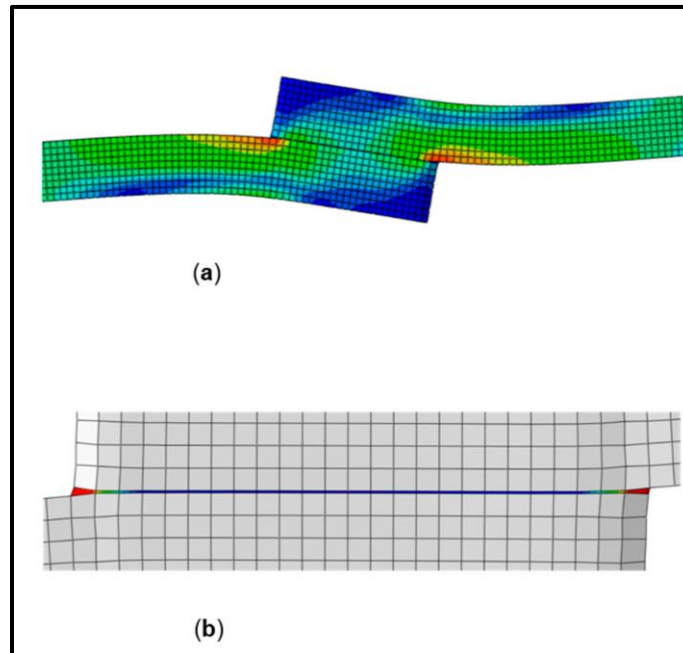
Below bar charts show a comparison between shear and peel stress at neat adhesive and filler induced adhesive at different weight percentages:
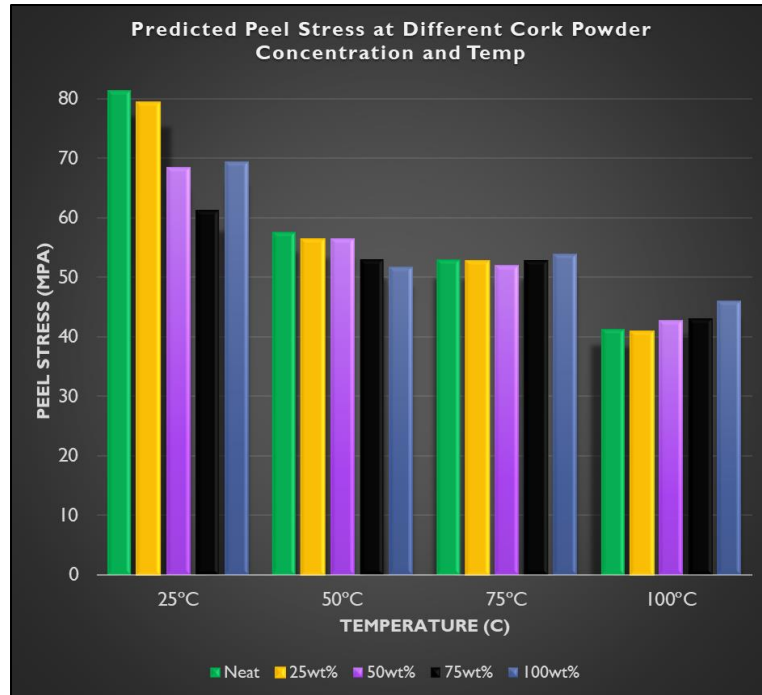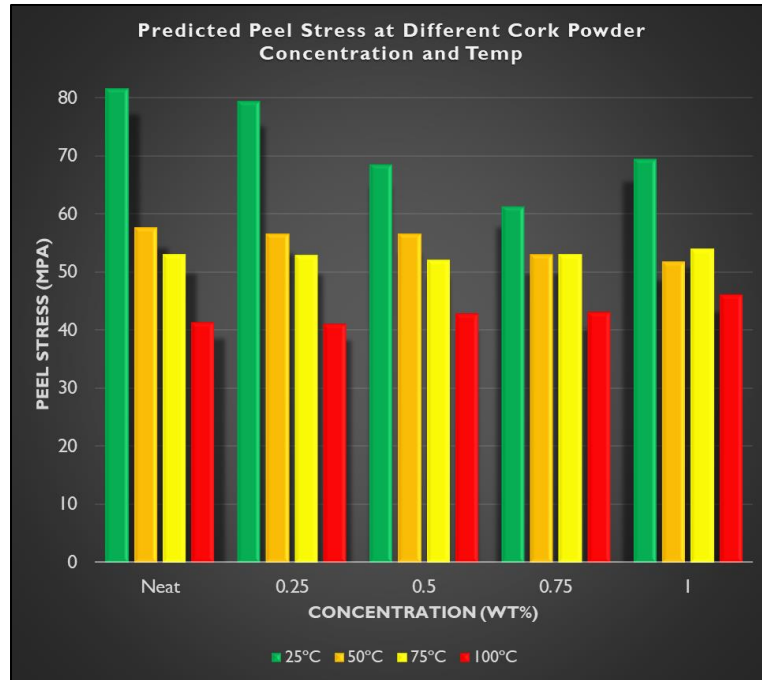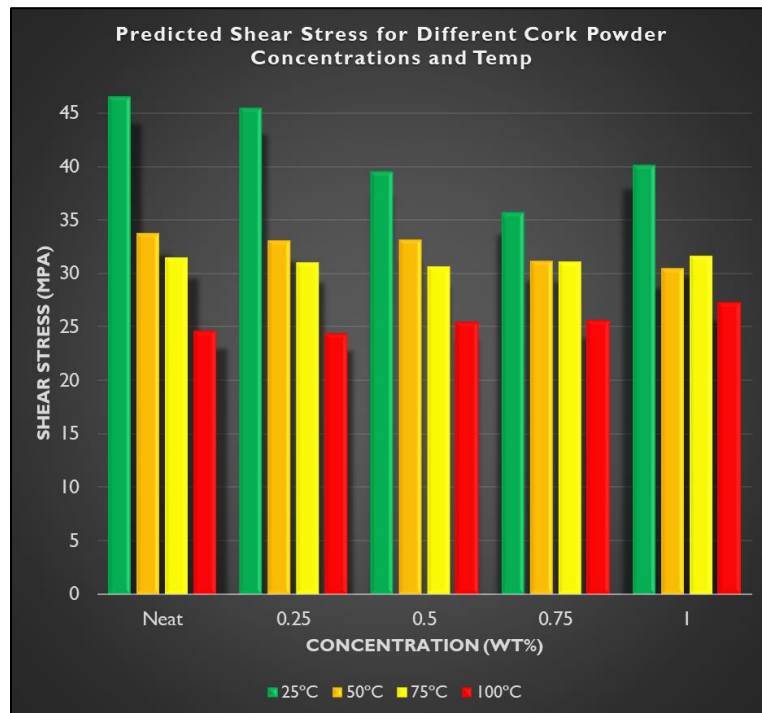
Chart 4.1: Bar Chart depicting Peel stress at all concentrations of cork powder
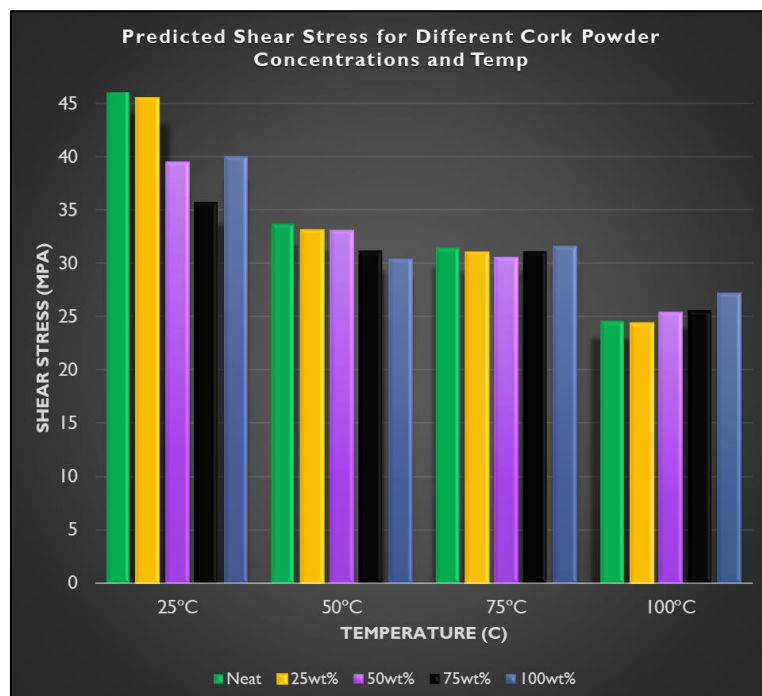
Chart 4.2: Bar Chart depicting Shear stress at all concentrations of cork powder 1

Chart 4.3: Bar Chart depicting Peel stress at all temperatures

Chart 4.4: Bar Chart depicting Shear stress at all temperatures

The overall behavior of the adhesive at different temperatures and concentrations can be summarized as:

a)   Peel stress reduces with increasing temperature at all cork powder concentrations. This tendency is predicted in adhesive systems, as high temperatures frequently result in decreased strength in many adhesive bonds. Higher temperatures may have an effect on the adhesive's integrity or the interaction between the adhesive and the substrate.

b)   The peel stress varies with cork powder content. Surprisingly, the peel stress at 0.25 wt% is somewhat lower than the neat adhesive at 25oC and 50oC, although it increases at higher temperatures (75oC and 100oC). This shows that, under certain conditions, only a small amount of cork powder may have a favorable influence on peel strength.

c)   Peel stress is often lower at 0.5 wt% cork powder compared to the neat adhesive, indicating that this concentration may not be optimum for boosting peel strength.

A linear regression analysis has been performed to predict the shear stress and peel stress (in MPa) based on several predictor variables. The regression model that has been used for peel and shear stress are:

Peel Stress:

$$\text{Peel Stress (MPa)} = 89.33 - 0.2236 \times \text{Cork Powder Concentration (wt\%)} - 0.5122 \times \text{Temperature (°C)} + 0.0030 \times \text{Interaction Term}$$

Intercept (Constant): 89.33

Coefficient for Cork Powder Concentration: -0.2236

Coefficient for Temperature: -0.5122

Coefficient for Interaction Term: 0.0030

R-squared: 0.8808

Mean Squared Error (MSE): 15.28

Shear Stress:

$$\text{Shear Stress (MPa)} = 50.92 - 0.1206 \times \text{Cork Powder Concentration (wt\%)} - 0.2802 \times \text{Temperature (°C)} + 0.0016 \times \text{Interaction Term}$$

Intercept (Constant): 50.92

Coefficient for Cork Powder Concentration: -0.1206

Coefficient for Temperature: -0.2802

Coefficient for Interaction Term: 0.0016

R-squared: 0.8861

Mean Squared Error (MSE): 4.36

In both these models, it can be concluded that Intercept (Constant) is the value of the peel and shear stress when all predictor variables are zero meaning that there is no participation of concentration or temperature. Negative coefficients of cork powder concentration suggest that with increase in concentration of the cork powder, shear and peel stresses increase. Negative coefficient for temperature suggests that every 25oC increase in temperature results in further reduction of the shear and peel stresses. Positive coefficient for the interaction term suggests that there is a positive interaction effect between the cork powder concentration and temperature on the peel and shear stress.

R-squared or coefficient of determination gives information regarding the wellness of the regression line against the actual data. An R-square of ~0.8 for both peel and shear stress tells that the independent variable has captured higher proportion of variability in the dependent variable. In this regression model, peel and shear stress are the dependent variables whereas cork powder concentration (wt%), Temperature (oC) and interaction term (product of concentration and temperature) are the independent terms.

Following plots show the linear regression model presenting the predicted and actual peel and shear stress values constituting a linear ascending pattern.
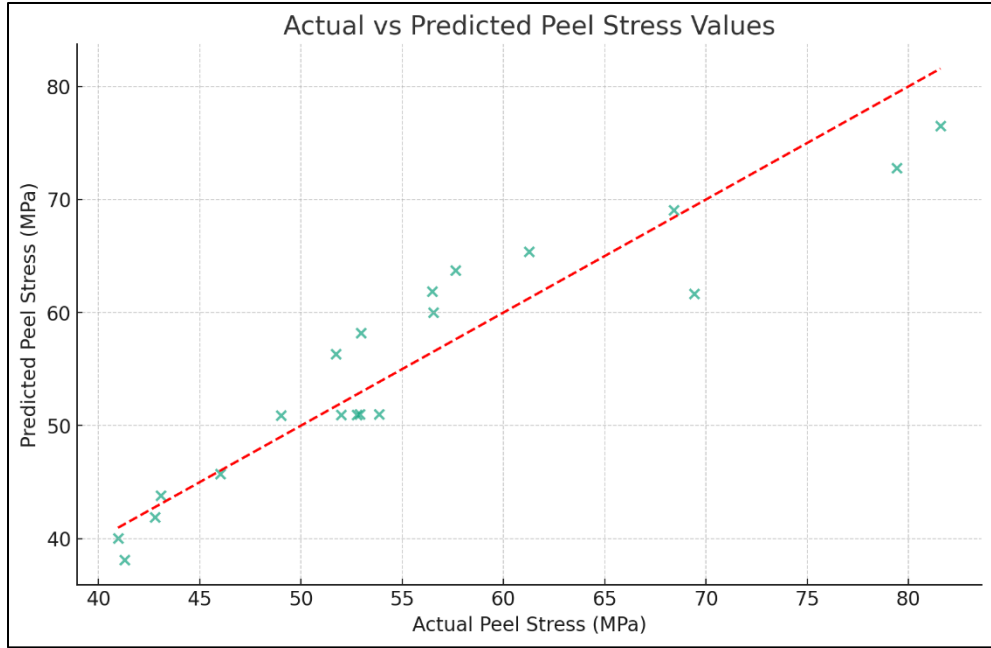
Graph 4.3: Linear Regression Model for Peel Stress
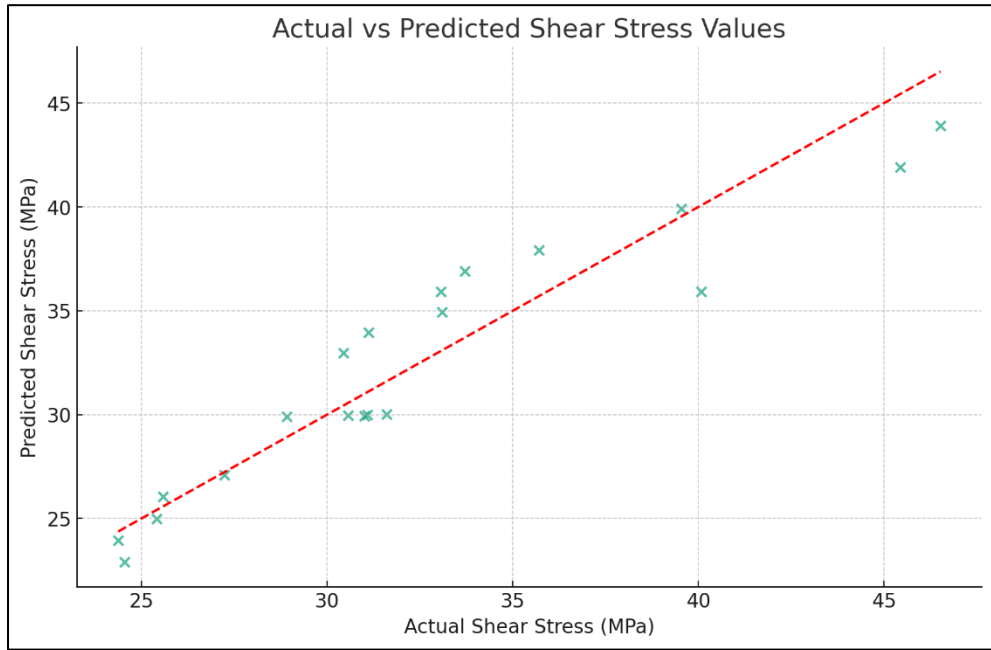
Graph 4.4: Linear Regression Model for Shear Stress

CHAPTER 5: CONCLUSION

The strength and failure mode of epoxy adhesives and single lap joint having aluminum adherend with brittle epoxy is evaluated using the experimented data and simulating by FEA analysis on Abaqus CAE. The simulation has been performed for 20 iterations that included: simulation of peel and shear stress for neat adhesive, 0.25.wt%, 0.5wt.%, 0.75.wt% and 100wt.% cork powder induced adhesive at four different temperatures of 25ºC, 50ºC, 75ºC and 100ºC. Following conclusions have been drawn from this study:

5.1 Adhesive Behavior:

• A particular quantity of cork particles appears to be optimum for the best adhesive ductility. (greater than 0.25wt% and less than 0.75wt%). Greater strength epoxy has less ductility and is more prone to be brittle.

• At 1wt%, the cork particles begin to behave flawed as the glue becomes more brittle.

• As the temperature rises over 50ºC, the epoxy glue appears to become more ductile as it approaches the glass transition point, resulting in increased strain to failure and lower tensile strength.

• As the temperature rises, the total tensile modulus of epoxy glue falls, implying that the stress-to-strain bearing ratio in epoxy adhesives diminishes.

5.2 Single Lap Joint (SLJ) Behavior:

• The addition of a particular amount of cork powder enhanced the loading capacity of adhesives.

• Cork may be described as a homogenous tissue with thin-walled cells that are uniformly arranged and devoid of intercellular spaces (similar to a honeycomb). When compared to brittle resin without particles, this cell shape improves epoxy adhesive's capacity to tolerate greater damage.

• However, only 0.5-0.75wt% increase may be adequate for these adhesives, and any more addition would impair SLAJ strength.

• The load displacement values of epoxy adhesives continue to climb somewhat until 0.5wt% and subsequently fall, suggesting that the specimen is losing loading capability.

5.3 Final Deductions from the Research:

• When a particular percentage of cork powder is applied, it serves as a crap stopper and boosts the overall ability of adhesives and SLJs to tolerate heavier loading.

• When 0.25 wt% and 0.5 wt% cork particles are introduced to brittle resin, they produce better ductility than 0.75 and 1 wt% cork. Cork powder acts worse than cork-free specimens at 1% because it begins to act like a defect at that point.

• Higher temperatures enhance the ductility of an adhesive joint, but the tensile strength and modulus of the glue are impaired.

• At temperatures closer to Tg, the strength of adhesives and joints is substantially reduced.

• As the temperature rises, the joint's failure mechanism switches from adhesive to cohesive failure.

REFERENCES

1. Adams, R.D., Comyn, J. and Wake, W.C., 1997. Structural adhesive joints in engineering. Springer Science & Business Media.

2. Adamvalli, M. and Parameswaran, V., 2008. Dynamic strength of adhesive single lap joints at high temperature. International Journal of Adhesion and Adhesives, 28(6), pp.321-327.

3. Ahmed, S. and Jones, F.R., 1990. A review of particulate reinforcement theories for polymer composites. Journal of materials science, 25, pp.4933-4942.

4. Al Mahmud, H., Radue, M.S., Chinkanjanarot, S. and Odegard, G.M., 2021. Multiscale modeling of epoxy-based nanocomposites reinforced with functionalized and non-functionalized graphene nanoplatelets. Polymers, 13(12), p.1958.

5. Alwar, R.S. and Nagaraja, Y.R., 1976. Elastic analysis of adhesive butt joints. The Journal of Adhesion, 7(4), pp.279-287.

6. Araújo, H.A.M., Machado, J.J.M., Marques, E.A.S. and Da Silva, L.F.M., 2017. Dynamic behaviour of composite adhesive joints for the automotive industry. Composite Structures, 171, pp.549-561.

7. Ashcroft, I.A., Hughes, D.J., Shaw, S.J., Wahab, M.A. and Crocombe, A., 2001. Effect of temperature on the quasi-static strength and fatigue resistance of bonded composite double lap joints. The Journal of Adhesion, 75(1), pp.61-88.

8. Banea, M.D., Rosioara, M., Carbas, R.J.C. and Da Silva, L.F.M., 2018. Multi-material adhesive joints for automotive industry. Composites Part B: Engineering, 151, pp.71-77.

9. Brooker, R.D., Kinloch, A.J. and Taylor, A.C., 2010. The morphology and fracture properties of thermoplastic-toughened epoxy polymers. The Journal of Adhesion, 86(7), pp.726-741.

10. Campilho, R.D., De Moura, M.F.S.F. and Domingues, J.J.M.S., 2005. Modelling single and double-lap repairs on composite materials. Composites Science and Technology, 65(13), pp.1948-1958.

11. Carneiro, M.A.S. and Campilho, R.D.S.G., 2017. Analysis of adhesively-bonded T-joints by experimentation and cohesive zone models. Journal of adhesion science and Technology, 31(18), pp.1998-2014.

12. Dorigato, A. and Pegoretti, A., 2011. The role of alumina nanoparticles in epoxy adhesives. Journal of Nanoparticle Research, 13, pp.2429-2441.

13. Fang, J., Sun, G., Qiu, N., Kim, N.H. and Li, Q., 2017. On design optimization for structural crashworthiness and its state of the art. Structural and Multidisciplinary Optimization, 55, pp.1091-1119.

14. Ferreira, F.V., Brito, F.S., Franceschi, W., Simonetti, E.A.N., Cividanes, L.S., Chipara, M. and Lozano, K., 2018. Functionalized graphene oxide as reinforcement in epoxy based nanocomposites. Surfaces and Interfaces, 10, pp.100-109.

15. Gao, Y., Picot, O.T., Bilotti, E. and Peijs, T., 2017. Influence of filler size on the properties of poly (lactic acid)(PLA)/graphene nanoplatelet (GNP) nanocomposites. European Polymer Journal, 86, pp.117-131.

16. Gupta, S.K., Shukla, D.K. and Bharti, A., 2017, February. Effect of alumina nanoparticles on shear strength of epoxy adhesive: experimental and finite element analysis. In 2017 International Conference on Advances in Mechanical, Industrial, Automation and Management Systems (AMIAMS) (pp. 307-313). IEEE.

17. Hassan, M., Mubashar, A., Masud, M., Zafar, A., Umair Ali, M. and Rim, Y.S., 2022. Effect of Temperature and Al2O3 NanoFiller on the Stress Field of CFRP/Al Adhesively Bonded Single-Lap Joints. Coatings, 12(12), p.1865.

18. He, X., 2011. A review of finite element analysis of adhesively bonded joints. International Journal of Adhesion and Adhesives, 31(4), pp.248-264.

19. Horstemeyer, M.F., 2010. Multiscale modeling: a review. Practical aspects of computational chemistry: methods, concepts and applications, pp.87-135.

20. Hsieh, T.H., Kinloch, A.J., Masania, K., Sohn Lee, J., Taylor, A.C. and Sprenger, S., 2010. The toughness of epoxy polymers and fibre composites modified with rubber microparticles and silica nanoparticles. Journal of materials science, 45, pp.1193-1210.

21. Hu, S., Jiang, H., Xia, Z. and Gao, X., 2010. Friction and adhesion of hierarchical carbon nanotube structures for biomimetic dry adhesives: multiscale modeling. ACS applied materials & interfaces, 2(9), pp.2570-2578.

22. Jairaja, R. and Naik, G.N., 2019. Single and dual adhesive bond strength analysis of single lap joint between dissimilar adherends. International Journal of Adhesion and Adhesives, 92, pp.142-153.

23. Karevan, M., Pucha, R.V., Bhuiyan, M.A. and Kalaitzidou, K., 2010. Effect of interphase modulus and nanofiller agglomeration on the tensile modulus of graphite nanoplatelets and carbon nanotube reinforced polypropylene nanocomposites. Carbon letters, 11(4), pp.325-331.

24. Kellar, E.J., 2021. Joining similar and dissimilar materials. In Adhesive bonding (pp. 385-405). Woodhead Publishing.

25. Khashaba, U.A., 2021. Dynamic analysis of scarf adhesive joints in CFRP composites modified with Al2O3-nanoparticles under fatigue loading at different temperatures. Composites Part A: Applied Science and Manufacturing, 143, p.106277.

26. Khashaba, U.A., Aljinaidi, A.A. and Hamed, M.A., 2014. Nanofillers modification of Epocast 50-A1/946 epoxy for bonded joints. Chinese Journal of Aeronautics, 27(5), pp.1288-1300.

27. Khashaba, U.A., Aljinaidi, A.A. and Hamed, M.A., 2015. Analysis of adhesively bonded CFRE composite scarf joints modified with MWCNTs. Composites Part A: Applied Science and Manufacturing, 71, pp.59-71.

28. Kinloch, A.J. and Taylor, A.C., 2006. The mechanical properties and fracture behaviour of epoxy-inorganic micro-and nano-composites. Journal of materials science, 41, pp.3271-3297.

29. Korta, J., Mlyniec, A. and Uhl, T., 2015. Experimental and numerical study on the effect of humidity-temperature cycling on structural multi-material adhesive joints. Composites Part B: Engineering, 79, pp.621-630.

30. Lee, C., Wei, X., Kysar, J.W. and Hone, J., 2008. Measurement of the elastic properties and intrinsic strength of monolayer graphene. science, 321(5887), pp.385-388.

31. Lubkin, J.L., 1957. A theory of adhesive scarf joints.

32. Marques, E.A.S., Da Silva, L.F., Banea, M.D. and Carbas, R.J.C., 2015. Adhesive joints for low-and high-temperature use: an overview. The Journal of Adhesion, 91(7), pp.556-585.

33. Morgado, M.A., Carbas, R.J.C., Dos Santos, D.G. and Da Silva, L.F.M., 2020. Strength of CFRP joints reinforced with adhesive layers. International Journal of Adhesion and Adhesives, 97, p.102475.

34. Mu, W., Qin, G., Na, J., Tan, W., Liu, H. and Luan, J., 2019. Effect of alternating load on the residual strength of environmentally aged adhesively bonded CFRP-aluminum alloy joints. Composites Part B: Engineering, 168, pp.87-97.

35. Nemati Giv, A., Ayatollahi, M.R., Ghaffari, S.H. and da Silva, L.F., 2018. Effect of reinforcements at different scales on mechanical properties of epoxy adhesives and adhesive joints: a review. The Journal of Adhesion, 94(13), pp.1082-1121.

36. Nguyen, T.C., Bai, Y., Al-Mahaidi, R. and Zhao, X.L., 2012. Time-dependent behaviour of steel/CFRP double strap joints subjected to combined thermal and mechanical loading. Composite structures, 94(5), pp.1826-1833.

37. Ostapiuk, M. and Bieniaś, J., 2019. Fracture analysis and shear strength of aluminum/CFRP and GFRP adhesive joint in fiber metal laminates. Materials, 13(1), p.7.

38. Qu, L., Dai, L., Stone, M., Xia, Z. and Wang, Z.L., 2008. Carbon nanotube arrays with strong shear binding-on and easy normal lifting-off. Science, 322(5899), pp.238-242.

39. Rahmani, A. and Choupani, N., 2019. Experimental and numerical analysis of fracture parameters of adhesively bonded joints at low temperatures. Engineering Fracture Mechanics, 207, pp.222-236.

40. Rahmani, A., Choupani, N. and Kurtaran, H., 2019. Thermo-fracture analysis of composite-aluminum bonded joints at low temperatures: Experimental and numerical analyses. International Journal of Adhesion and Adhesives, 95, p.102422.

41. Reis, P.N., Ferreira, J.A.M. and Antunes, F., 2011. Effect of adherend's rigidity on the shear strength of single lap adhesive joints. International Journal of Adhesion and Adhesives, 31(4), pp.193-201.

42. Ribeiro, T.E.A., Campilho, R.D.S.G., da Silva, L.F. and Goglio, L., 2016. Damage analysis of composite–aluminium adhesively-bonded single-lap joints. Composite Structures, 136, pp.25-33.

43. Rothon, R.N. and Hancock, M., 1995. General principles guiding selection and use of. Particulate-filled polymer composites, p.1.

44. Salom, C., Prolongo, M.G., Toribio, A., Martínez-Martínez, A.J., de Cárcer, I.A. and Prolongo, S.G., 2018. Mechanical properties and adhesive behavior of epoxy-graphene nanocomposites. International Journal of Adhesion and Adhesives, 84, pp.119-125.

45. Sanghvi, M.R., Tambare, O.H. and More, A.P., 2022. Performance of various fillers in adhesives applications: A review. Polymer Bulletin, 79(12), pp.10491-10553.

46. Scarselli, G., Corcione, C., Nicassio, F. and Maffezzoli, A., 2017. Adhesive joints with improved mechanical properties for aerospace applications. International journal of adhesion and adhesives, 75, pp.174-180.

47. Shang, X., Marques, E.A.S., Machado, J.J.M., Carbas, R.J.C., Jiang, D. and Da Silva, L.F., 2019. Review on techniques to improve the strength of adhesive joints with composite adherends. Composites Part B: Engineering, 177, p.107363.

48. Sheng, N., Boyce, M.C., Parks, D.M., Rutledge, G.C., Abes, J.I. and Cohen, R.E., 2004. Multiscale micromechanical modeling of polymer/clay nanocomposites and the effective clay particle. Polymer, 45(2), pp.487-506.

49. Stankovich, S., Dikin, D.A., Dommett, G.H., Kohlhaas, K.M., Zimney, E.J., Stach, E.A., Piner, R.D., Nguyen, S.T. and Ruoff, R.S., 2006. Graphene-based composite materials. nature, 442(7100), pp.282-286.

50. Steinhauser, M.O., 2017. Computational multiscale modeling of fluids and solids. Berlin: Springer.

51. Suárez, J.C., de Ulzúrrun, I.D., Biezma, M.V., Román, J.R., Martínez, M.A., Del Real, J.C. and López, F., 2003. Case studies in adhesives selection. Journal of materials processing technology, 143, pp.219-224.

52. Sun, L., Li, C., Tie, Y., Hou, Y. and Duan, Y., 2019. Experimental and numerical investigations of adhesively bonded CFRP single-lap joints subjected to tensile loads. International Journal of Adhesion and Adhesives, 95, p.102402.

53. Sydlik, S.A., Lee, J.H., Walish, J.J., Thomas, E.L. and Swager, T.M., 2013. Epoxy functionalized multi-walled carbon nanotubes for improved adhesives. Carbon, 59, pp.109-120.

54. Taheri, F., 2020. Improvement of the performance of structural adhesive joints with nanoparticles and numerical prediction of their response. Structural Adhesive Joints: Design, Analysis and Testing, pp.35-78.

55. Thabet, A., Mubarak, Y.A. and Bakry, M.J.J.E.S., 2011. A review of nano-fillers effects on industrial polymers and their characteristics. J. Eng. Sci, 39, pp.377-403.

56. Upadhyaya, P., Kumar, S., Reddy, J.N. and Lacy Jr, T.E., 2020. Multiscale modeling of strength and failure behavior of carbon nanostructure reinforced epoxy composite adhesives in bonded systems. European Journal of Mechanics-A/Solids, 80, p.103932.

57. Utracki, L.A., 2013. Commercial polymer blends. Springer Science & Business Media.

58. Van Der Giessen, E., Schultz, P.A., Bertin, N., Bulatov, V.V., Cai, W., Csányi, G., Foiles, S.M., Geers, M.G., González, C., Hütter, M. and Kim, W.K., 2020. Roadmap on multiscale materials modeling. Modelling and Simulation in Materials Science and Engineering, 28(4), p.043001.

59. Vanorio, T., Prasad, M. and Nur, A., 2003. Elastic properties of dry clay mineral aggregates, suspensions and sandstones. Geophysical Journal International, 155(1), pp.319-326.

60. Wang, S., Liang, W., Duan, L., Li, G. and Cui, J., 2020. Effects of loading rates on mechanical property and failure behavior of single-lap adhesive joints with carbon fiber reinforced plastics and aluminum alloys. The International Journal of Advanced Manufacturing Technology, 106, pp.2569-2581.

61. Zare, Y., 2015. Effects of interphase on tensile strength of polymer/CNT nanocomposites by Kelly–Tyson theory. Mechanics of Materials, 85, pp.1-6.

62. Zhou, Y., Pervin, F. and Jeelani, S., 2007. Effect vapor grown carbon nanofiber on thermal and mechanical properties of epoxy. Journal of Materials Science, 42, pp.7544-7553.

63. Zuberi, M.J.S. and Esat, V., 2015. Investigating the mechanical properties of single walled carbon nanotube reinforced epoxy composite through finite element modelling. Composites Part B: Engineering, 71, pp.1-9.